

Analysis of Li-ion Kinetics in LFP Cylindrical Cells Using Electrochemical Impedance Spectroscopy



By

Syed Maaz Bin Qamar

Registration No: 00000363229

Department of Energy Systems Engineering

US Pakistan Center for Advanced Studies in Energy (USPCAS-E)

National University of Sciences & Technology (NUST)

Islamabad, Pakistan

(2024)

Analysis of Li-ion Kinetics in LFP Cylindrical Cells Using Electrochemical Impedance Spectroscopy



By

Syed Maaz Bin Qamar

(Registration No: 00000363229)

A thesis submitted to the National University of Sciences and Technology, Islamabad,

In partial fulfillment of the requirements for the degree of

Master of Science in
Energy Systems Engineering

Supervisor: Dr. Ghulam Ali

US Pakistan Center for Advanced Studies in Energy (USPCAS-E)

National University of Sciences & Technology (NUST)

Islamabad, Pakistan

(2024)

THESIS ACCEPTANCE CERTIFICATE

Certified that final copy of MS Thesis written by Mr. Syed Maaz Bin Qamar (Registration No. 00000363229), of Department of Energy Systems Engineering, School of U.S Pakistan Center for Advanced Studies in Energy, National University of Sciences & Technology (NUST) Islamabad, Pakistan, has been vetted by undersigned, found complete in all respects as per NUST Statutes/ Regulations/ Masters Policy, is free of plagiarism, errors, and mistakes and is accepted as partial fulfillment for award of master's degree. It is further certified that necessary amendments as pointed out by GEC members and foreign/ local evaluators of the scholar have also been incorporated in the said thesis.


Signature: 

Name of Supervisor: Dr. Ghulam Ali

Date: 18-12-2024

Signature (HOD): 

Date: 19-12-2024

Signature (Dean/ Principal) 

Date: 20/12/2024

National University of Sciences & Technology
MASTER'S THESIS WORK

We hereby recommend that the dissertation prepared under our supervision by
Syed Maaz Bin Qamar; 00000363229

Titled: Analysis of Li-ion Kinetics in LFP Cylindrical Cells Using Electrochemical Impedance Spectroscopy (EIS) be accepted in partial fulfillment of the requirements for the award of **MS Energy Systems Engineering** degree with (A) grade.

Examination Committee Members


1. Name: Dr. Mustafa Anwar

Signature: 

2. Name: Dr. Syed Ali Abbas Kazmi

Signature: 

3. Name: Dr. Muhammad Yousif

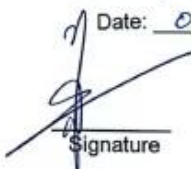
Signature: 

Supervisor's name: Dr. Ghulam Ali

Signature: 

Date: 06-12-2024

Dr. Naseem Iqbal
Head of Department


Signature

19-12-2024
Date

COUNTERSIGNED

Date: 20/12/24


Dean/Principal

CERTIFICATE OF APPROVAL

This is to certify that the research work presented in this thesis, entitled "Analysis of Li-ion Kinetics in LFP Cylindrical Cells Using Electrochemical Impedance Spectroscopy" was conducted by Mr./Miss Syed Maaz Bin Qamar under the supervision of Dr. Ghulam Ali.

No part of this thesis has been submitted anywhere else for any other degree. This thesis is submitted to the Department of Energy Systems Engineering in partial fulfillment of the requirements for the degree of Master of Science in Field of Energy Storage. Department of Energy Systems Engineering, National University of Sciences and Technology, Islamabad.

Student Name: Syed Maaz Bin Qamar

Signature: 

Examination Committee:

a) GEC Member 1: Dr. Mustafa Anwar
(Assistant Professor, USPCAS-E NUST)

Signature: 

b) GEC Member 2: Dr. S. A. A. Kazmi
(Associate Professor, USPCAS-E NUST)

Signature: 

c) GEC Member 3: Dr. M. Yousif
(Assistant Professor, USPCAS-E NUST)

Signature: 

Supervisor Name: Dr. Ghulam Ali

Signature: 

Name of HOD: Dr. Naseem Iqbal

Signature: 

Name of Principal/Dean: Dr. Adeel Waqas

Signature: 

AUTHOR'S DECLARATION

I, Syed Maaz Bin Qamar, hereby state that my MS thesis titled "Analysis of Li-ion Kinetics in LFP Cylindrical Cells Using Electrochemical Impedance Spectroscopy" is my own work and has not been submitted previously by me for taking any degree from the National University of Sciences and Technology, Islamabad or anywhere else in the country/ world.

At any time if my statement is found to be incorrect even after I graduate, the university has the right to withdraw my MS degree.

Name of Student: Syed Maaz Bin Qamar

Date: 18-12-24

PLAGIARISM UNDERTAKING

I solemnly declare that the research work presented in the thesis titled “Analysis of Li-ion Kinetics in Cylindrical LFP Cells Using Electrochemical Impedance Spectroscopy” is solely my research work with no significant contribution from any other person. Small contribution/ help wherever taken has been duly acknowledged and that complete thesis has been written by me.

I understand the zero-tolerance policy of the HEC and the National University of Sciences and Technology (NUST), Islamabad towards plagiarism. Therefore, I as an author of the above titled thesis declare that no portion of my thesis has been plagiarized and any material used as reference is properly referred/cited.

I undertake that if I am found guilty of any formal plagiarism in the above titled thesis even after the award of MS degree, the University reserves the rights to withdraw/revoke my MS degree and that HEC and NUST, Islamabad has the right to publish my name on the HEC/University website on which names of students are placed who submitted plagiarized thesis.

Student Signature: Maaz

Name: Syed Maaz Bin Qamar

DEDICATION

This thesis is dedicated first to my beloved parents for their love, support, and affection. Then to my dedicated and hardworking Supervisor for his kind support throughout my research. This achievement is as much as yours as it is mine. Thank you all for being my pillars of strength and confidence.

ACKNOWLEDGMENTS

I would like to thank my Supervisor **Dr. Ghulam Ali** from the bottom of my heart for his trustworthiness in my abilities and for his continuous support throughout the time of my research work. The commitment and the support he showed me with all his love and affection will stay with me for the rest of my life.

I would like to thank my parents for their unequivocal support and to back me up in times of difficulties.

Lastly, all the support and help I received from my lab colleagues, specifically, **Abdullah Javaid, Khadija Nasir, Haseeb Ahmad,** and **Deepak Kumar** will always remain in my heart. I would like to say thank you to all the Lab Assistants, Friends, and GEC members for their guidance and support during my MS Degree.

TABLE OF CONTENTS

ACKNOWLEDGMENTS	ix
TABLE OF CONTENTS	x
LISTS OF FIGURES	xii
LIST OF TABLES	xiv
LIST OF ABBREVIATIONS, ACRONYMS, AND ACRONYMS	xv
ABSTRACT	xvi
CHAPTER 1: INTRODUCTION	1
1.1 BACKGROUND INFORMATION	1
1.1.1 Fossil fuel and its disadvantages.....	1
1.1.2 Renewable Energy and its advantages.....	3
1.1.3 Problems with Renewable Energy	5
1.1.4 Battery as an Energy Storage Device.....	6
1.1.5 Lithium-ion Cell Working.....	7
1.1.6 Lithium Iron Phosphate (LFP) and its advantages.....	10
1.1.7 Degradation of cell analyzed through EIS	11
1.1.8 Effect of Temperature and C-rate on Degradation.....	12
1.2 Problem Statement	13
1.3 Research Hypothesis	14
1.4 Objective	14
1.5 Scope of the Study	14
1.6 Summary	15
CHAPTER 2: LITERATURE REVIEW	16
2.1 Literature	16
2.2 Summary	20
CHAPTER 3: Review of Experimental & Characterization Work	21
3.1 Battery Analyzer	21
3.1.1 Testing Conditions	22
3.1.1.1 Constant Current Charging	22
3.1.1.2 Constant Voltage Charging	23
3.1.1.3 Constant Current & Constant Voltage (CC-CV) Charge	23
3.2 Electrochemical Impedance Spectroscopy (EIS)	24

3.2.1 Working.....	25
3.3 Thermally Insulated Chamber or Environmental Chamber.....	26
3.3.1 PTC Element.....	26
3.3.2 W1209 Temperature Controller	27
3.3.3 NTC Sensor.....	28
3.3.4 Monitoring System.....	29
3.3.5 k-type Thermocouple	29
3.3.6 Data Logger	30
3.4 Summary.....	31
CHAPTER 4: Experimental Methodology.....	32
4.1 Tested Cells	32
4.2 Battery Analyzer, Electrochemical Impedance Spectroscopy (EIS), & Thermal Chamber setup:.....	32
4.3 Cyclic Protocols:.....	33
4.4 Summary.....	34
CHAPTER 5: Results and Discussion:	35
5.1 EIS study before cycling or 0 th cycle	35
5.2 EIS testing after 1 st cycle	36
5.3 EIS testing after 100 th cycle.....	38
5.4 EIS comparison after 400 th cycle	40
5.5 EIS after various State of Charges (SOCs).....	43
5.6 Diffusion Studies with respect to cycling of the cell cycled at 2.5 C at room temperature	46
5.7 Diffusion studies at various c-rates	49
5.8 Summary.....	51
CHAPTER 6: Conclusion and Future Recommendation	52
6.1 Conclusion	52
6.2 Limitations.....	53
6.3 Future Recommendations	53
REFERENCES.....	55
LIST OF PUBLICATION	64

LISTS OF FIGURES

Figure 1.1: Amount of fossil fuels consumed based on global level [2].	2
Figure 1.2: Renewable energy mix by generation in the world [9].	4
Figure 1.3: Types of Renewable Energy Sources [10].	4
Figure 1.4: Problems with renewable energy supplies [13].	5
Figure 1.5: Types of Energy Storage Systems and their applications [15].	6
Figure 1.6: Lithium-ion battery pack along with its components [18].	7
Figure 1.7: Lithium-ion cell components and their possible structures [21].	8
Figure 1.8: Charging process of lithium-ion cell and the flow of charges are depicted [21].	9
Figure 1.9: Discharging process of lithium-ion cell and flow of charges [21].	9
Figure 1.10: Types of Li-ion battery chemistries and their features[22].	10
Figure 1.11: EIS and its valuable information extraction [28].	12
Figure 1.12: Effects of temperature and c-rates on Li-ion battery [29].	13
Figure 3.1: Battery Analyzer setup with its connections [60].	21
Figure 3.2: Various charging methods shown including Constant Current & Constant Voltage Charging [64].	23
Figure 3.3: The CC-CV charging settings shown on a battery analyzer [7].	24
Figure 3.4: Nyquist plot along with equivalent circuit model derived from EIS test [67].	25
Figure 3.5: A PTC device with aluminium body for heat uniformity [69].	27
Figure 3.6: A W1209 temperature controller with its components labelling [71].	28
Figure 3.7: An NTC sensor used in W1209 temperature controller [73].	29
Figure 3.8: k-type Thermocouple with its two legs [75].	30
Figure 3.9: Digital Data Logger	31
Figure 4.1: self-made environmental chamber to perform all experiment at 55 °C.	34
Figure 5.1: EIS testing before cycling at a) room temperature and b) 55 °C	36
Figure 5.2: EIS testing after 1st cycle at a) room temp. b) 55 °C temperature. Equivalent circuits shown for cells cycled at 55 °C temp. at c) 0.5 C to 1.5 C d) 2 C e) 2.5 C	38
Figure 5.3: EIS comparison of cell cycled for 100 cycles at a) room temp. b) 55 °C temp. c) Equivalent circuit obtained for room temp. study d) Equivalent circuit obtained for 55 °C temp. study	39

Figure 5.4: EIS comparison after 400th cycle at **a)** room temp. **b)** 55 °C temp.43

Figure 5.5: EIS study at various SOCs **a)** SOC vs. Volt. **b)** SOCs after 1st cycle at 0.5 C **c)** SOCs after 400th cycle at 2.5 C45

Figure 5.6: Diffusion Coefficient at 2.5 C, room temp. after **a)** 1st cycle **b)** 100th cycle **c)** 400th cycle.48

Figure 5.7: Diffusion Coefficient of cell **a)** without cycling. For cells cycled for 400 cycles **b)** at 0.5 C **c)** at 1 C **d)** at 1.5 C **e)** at 2 C..... 50

LIST OF TABLES

Table 4.1: Lithium-ion Iron Phosphate (LFP) commercial cell of 18650 model with their specifications provided by Akkuteile manufacturers.....	32ss
Table 5.1: Summary of R_{ct} values obtained from this study at different temperatures, different c-rates, and various number of cycles.....	41
Table 5.2: Summary of R_s and R_E values obtained from this study at different temperatures, different c-rates, and various number of cycles.....	42

LIST OF ABBREVIATIONS, ACRONYMS AND ACRONYMS

Nomenclature

LFP	Lithium Iron Phosphate
EIS	Electrochemical Impedance Spectroscopy
GITT	Galvanostatic Intermittent Titration Technique
SOC	State of Charge
SOH	State of Health
SOF	State of Function
CC	Constant Current
CV	Constant Voltage
CCCV	Constant Current Constant Voltage
SEI	Solid Electrolyte Interface

Symbols

$^{\circ}\text{C}$	Degree Centigrade
D	Diffusion Coefficient
R_s	Solution Resistance
R_e	Equivalent Resistance
C_{PE}	Constant Phase Element
R_{ct}	Charge Transfer Resistance

Greek Letters

Ω	Ohm
σ	Slope
π	Pi
ω	Omega

ABSTRACT

The Lithium-ion cell is a highly complex electrochemical device which needs further study to better understand its kinetics and its degradation mechanisms for its wider applicability and useability. The lack of understanding of how external factors influence this electrochemical device hinders its operating limits. To study how and in what way these factors influence their performance and affect their behavior, an electrochemical impedance spectroscopy (EIS) technique was utilized to comprehend this phenomenon. The external temperature, the cyclability, the charge/discharge rate and the influence of State of Charge (SOC) was used to study the kinetics parameters and the degradational mechanisms. The outcomes studied were charge-transfer resistance R_{ct} , solution resistance R_s , and the diffusion coefficient D . The study figured out that the cyclability enhances the charge transfer events as it improves the diffusional pathways. The correlation with diffusion coefficient was investigated and proved to be true. The effects of temperature and c-rates were also found to be of importance when investigating the kinetic parameters. The dependency of charge-discharge rates on solution resistance was found beneficial as it highlighted various degradation mechanisms often ignored in search of charge transfer relationship. The role of SOC highlighted the fact that cycling at lower SOC's contributes towards SEI formation and had more detrimental impact as compared to the cells cycled at higher SOC's. However, each parameter affected the cell in its own way as some were found to be detrimental upon their increase while some affect the cell upon their smaller values. These variations in trends give beneficial information regarding the activities and operating limits of the lithium-ion batteries (LIBs). Henceforth, the EIS proves to be an effective tool for deciphering the kinetics and degradational behavior of the cells.

Keywords: Lithium-ion battery, Charge Transfer Resistance, Diffusion coefficient, Solution Resistance, State of Charge, Solid Electrolyte Interface, Electrochemical Impedance Spectroscopy

CHAPTER 1: INTRODUCTION

1.1 BACKGROUND INFORMATION

This study starts with touching upon important foreground information regarding the need for Li-ion batteries and why they are important.

1.1.1 Fossil fuel and its disadvantages

The world today is facing a humungous challenge of global warming and climate change. It is facing such consequences due to widespread use of fossil fuels in our daily life. A report of UN mentions that if measures are not taken early, the Earth could see doubled the temperature rise of 1.5 °C [1]. This alarming situation calls for swift and logical actions that needs to be taken to avoid catastrophic events. To tackle the problem of climate change, the core of the problem should be understood. Hence, the main problem causing this sudden temperature rise are the fossil fuels which are deeply engraved in our daily activities. From electricity running our appliances to transportation taking us here and there, everything runs on fossil fuels. Fossil fuels are the hydrocarbon sources from living beings which were fossilized after remaining buried inside the earth or a mountain for millions of years. They are usually extracted and utilized in the form of coal, gas, and oil. Though there exist many other types of fossil fuels, these three are the primary sources.

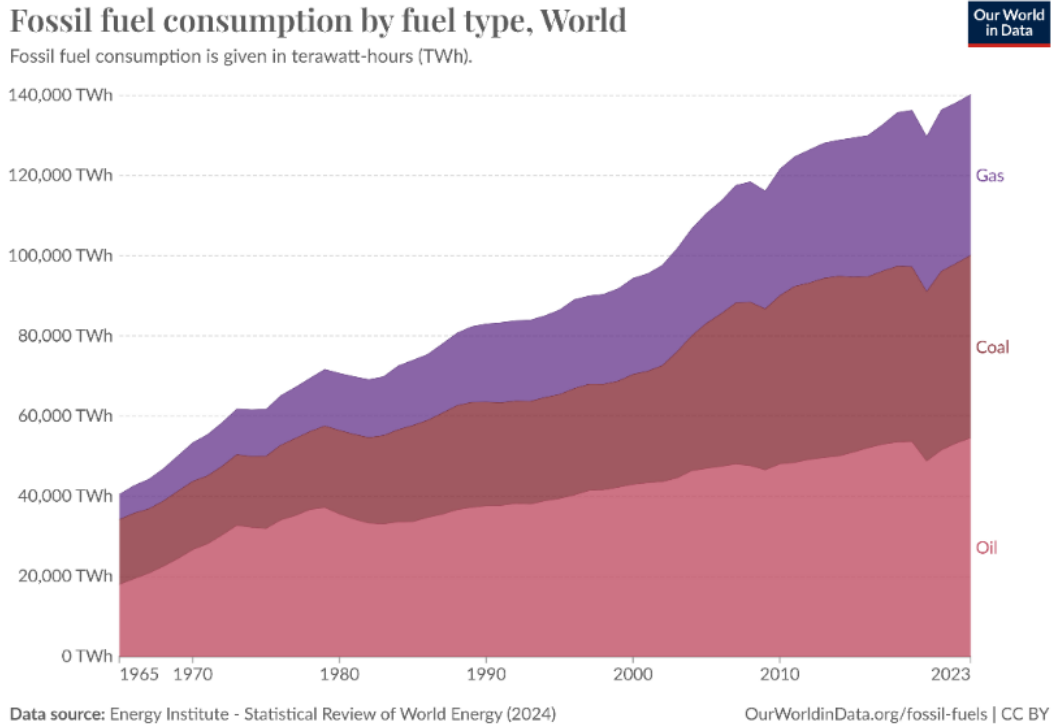


Figure 1.1: Amount of fossil fuels consumed based on global level [2].

A report published by Energy Institute-Statistical Review of World Energy (2024) indicates that the total fossil fuel consumption, aggregately on a global scale, makes up about one fifty thousand Terawatt-hours. The figure 1.1 indicates that Oil has the largest share in global energy mix (around 55k TWh) followed by coal and gas, respectively [3].

As for Pakistan, the energy resources in Pakistan are diminishing day-by-day on one side and its demand is increasing on the other side. Pakistan’s energy mix consists of about 65% fossil fuels [4], which can contribute large amount of greenhouse gas emission in the country. From the production of electricity and cement factories alone, the CO₂ emissions from fossil fuels as reported in 2022 data was about 200 million tons [5]. This staggering number speaks volumes when it comes to mitigating the effects of climate change.

From mining till burning, every process involved in the fossil fuels contributes to some kind of pollution. The disadvantages of fossil fuels are many which includes greenhouse gas (GHG) emissions, carbon dioxide (CO₂) emission, air, land, and water pollution, limitations in its

availability, and causes ozone layer depletion. These are some of the major adversarial effects of fossil fuels on our environment and global temperatures [6].

1.1.2 Renewable Energy and its advantages

Since fossil fuels have negative effects on our world and they are also a depleting source, there was an urgent need to switch towards something which is long-lasting and is safer for the environment.

Renewable energy sources serve the exact purpose of providing a naturally driven, abundant source of energy extracted from the environment and are also significantly better for the environment. Renewable energy sources extract energy from multiple aspects of the environment which includes sun, wind, water, tides, waves, and biomass [7].

As compared to fossil fuels, renewable energy sources are everlasting, environmental-friendly, cheaper, and produces less emissions during their manufacturing and generating processes[8]. This makes them a suitable replacement for the fossil fuels which are causing vast amount of damage to the world.

Renewable electricity generation, World

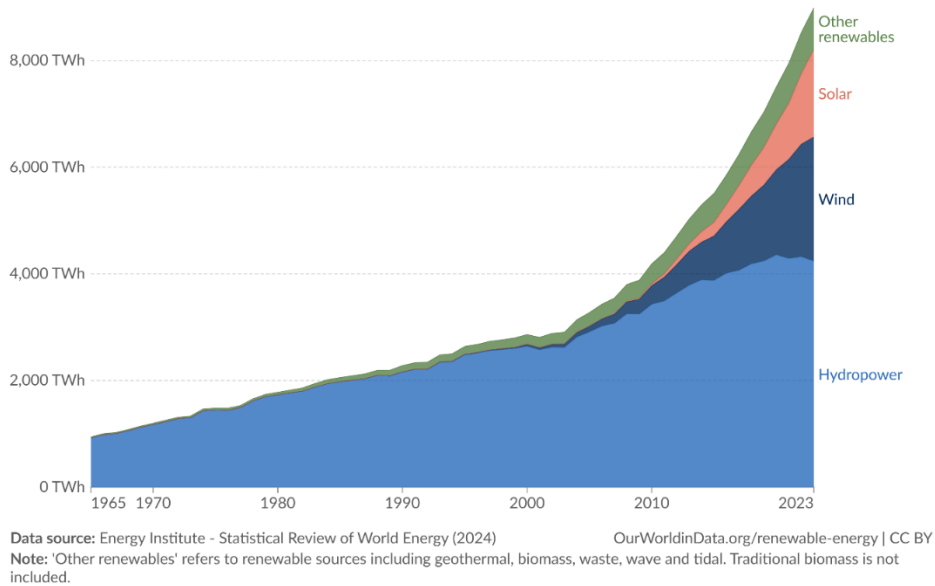


Figure 1.2: Renewable energy mix by generation in the world [9]

As seen from figure 1.2, the total renewable energy mix by 2023 in the world has increased to about 9000 Terawatt-hours as compared to around 4000 TWh in 2010. In almost all the years, the share of hydropower is the largest with about four thousand terawatt-hour in 2023 while that of other renewable sources like biomass and tidal energy contributes the lowest.



Figure 1.3: Types of Renewable Energy Sources [10]

1.1.3 Problems with Renewable Energy

In order to mitigate the effects of climate change, there is an urgent need to switch towards renewable energy sources and to introduce them into Pakistan's energy mix. There are many renewable sources being used like Solar, Wind, Hydro etc., however, they can't meet the energy demands all the time [11]. Henceforth, a sustainable renewable energy system is required for their wider application.

Since renewable energy sources are dependent upon natural sources like Sun, wind, etc., they have intermittency and stability issues. For example, the PV technology requires continuous sunlight in order to operate efficiently while Wind turbines require a certain speed for the turbines to move and generate electricity [8][12]. Therefore, the applicability of renewable energy sources is hindered by their lack of sustainability and predictability.

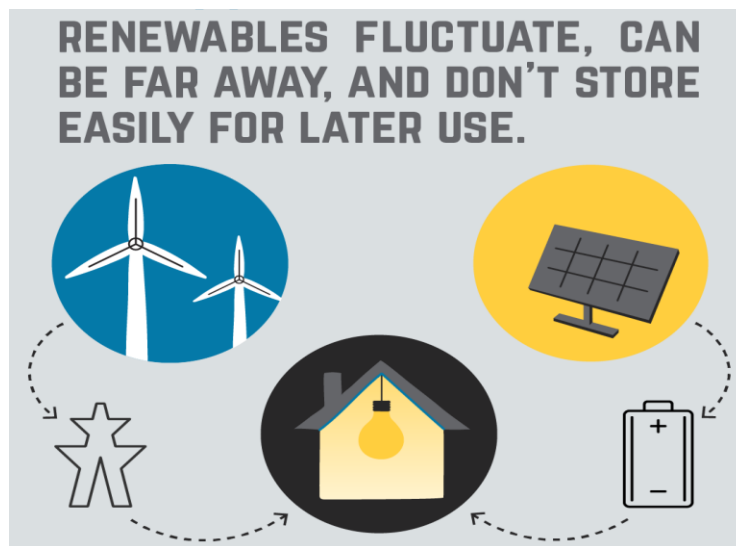


Figure 1.4: Problems with renewable energy supplies [13].

To overcome the problem of intermittency and availability as shown in figure 1.4, an energy storage system must be implemented with renewable energy sources. There are many kinds of energy storage systems, and they vary based on their mechanisms and scalability, the battery storage system is discussed below as a viable option for this discussion.

1.1.4 Battery as an Energy Storage Device

Energy storage systems are the ones which can provide sustainability to renewable energy sources. Batteries are one of the energy storage systems which are rapidly expanding in providing huge capacity in its storage [14]. There are many types of batteries which are being utilized with varying cycle life, voltage levels, and costs as shown in figure 1.5. However, Lithium-ion batteries are the most widely used energy storage system which stands out from the rest.

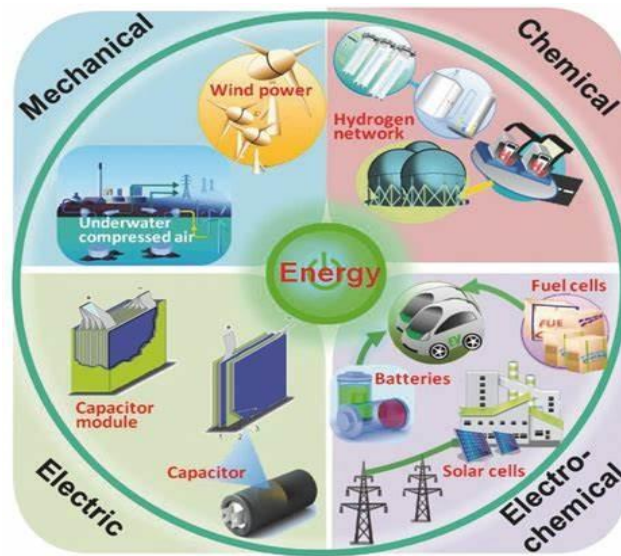


Figure 1.5: Types of Energy Storage Systems and their applications [15].

Lithium-ion batteries possess longer cycle life, higher voltage levels, and are being produced more cheaply day-by-day. They have higher energy density and are more environmental-friendly as compared to other types of batteries [16].

Lithium-ion cell possesses a higher specific capacity of about 3.86 Ah/g and possess a large energy density as compared to other types of batteries. The cycle life of Li-ion batteries is longer than 1000 cycles due to their stable structures and mechanisms [17]. These advantages give them the upper hand in their applicability and widespread usage.

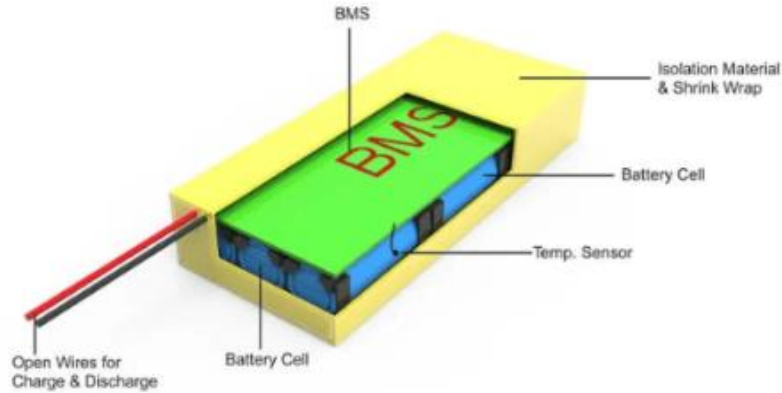


Figure 1.6: Lithium-ion battery pack along with its components [18].

1.1.5 Lithium-ion Cell Working

Lithium-ion cells consist of an Anode, Cathode, Electrolyte, and Separator. These cell components make up the full-cell configuration. The cells are then connected to make a battery pack which can handle large loads. The electrodes, i.e., cathode and anode, serves as reaction sites and allows for Lithium-ion to intercalate/de-intercalate. The figure 1.7 shows the parts of a lithium-ion cell and their structures for better visualization [19].

The cathode is made by lithium metal oxides while anode consists of lithium carbon compounds. The cathodic material supplies the lithium ions while anode electrode serves as storage site for these ions. The electrolyte serves as a diffusion channel for the ions while the separator avoids unnecessary contact between the electrodes and electrolytes [20].

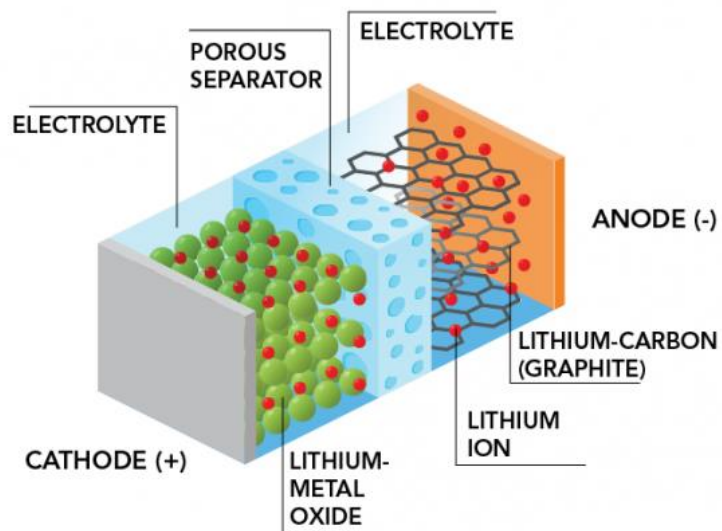


Figure 1.7: Lithium-ion cell components and their possible structures [21]

The cell works by the movement of lithium ions between the electrodes and flow of electrons from the outer circuit. Since cathode produces the lithium ions, during charging process, the Li^+ ion moves from the cathode and intercalates into the anode as shown in figure 1.8. While on discharging, the opposite mechanism occurs with lithium ion moving from anode to cathode and the electrons flowing through the load from the outer circuit as shown in figure 1.9.

CHARGING

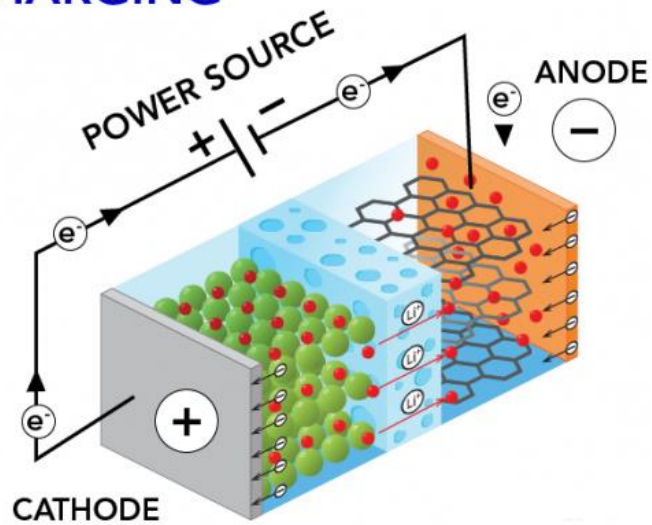


Figure 1.8: Charging process of lithium-ion cell and the flow of charges are depicted [21].

DISCHARGING

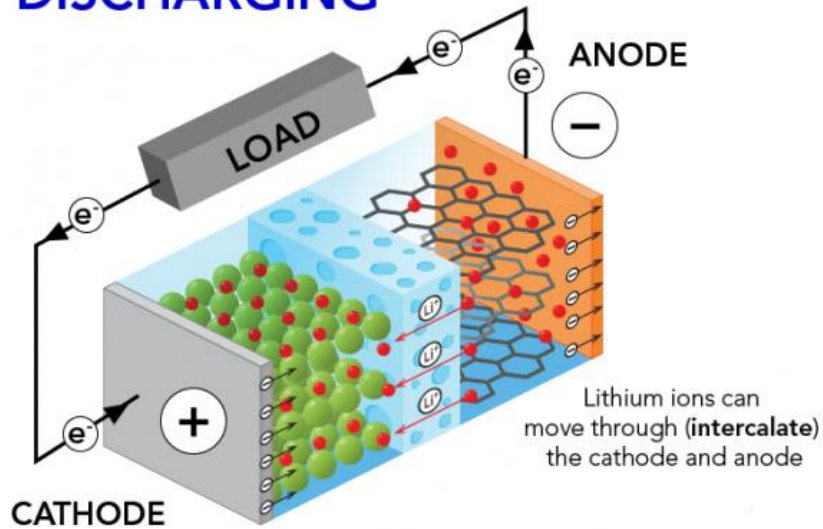
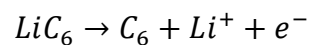
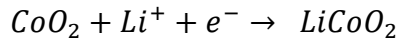


Figure 1.9: Discharging process of lithium-ion cell and flow of charges [21]

At the anode side, oxidation reaction occurs during charging as Li-ions move towards the anode from cathode. For LiCoO_2 cell, the oxidation reaction looks like this:



On the other hand, reduction reaction takes place at cathode side while discharging as Li^+ move from anode to cathode. For LiCoO_2 cell, the reduction reaction looks like this:



1.1.6 Lithium Iron Phosphate (LFP) and its advantages

There are many types of Li-ion chemistries which are either commercialized or about to be commercialized in the market. Every Li-ion battery chemistry is unique in various ways. Some have better energy density or the ability to store more energy per unit weight while others have better power density or the ability to supply large amount of current. These two are primary factors but there are other ways in which a Li-ion chemistry can differ like voltage-level, safety level, number of cycles, etc.

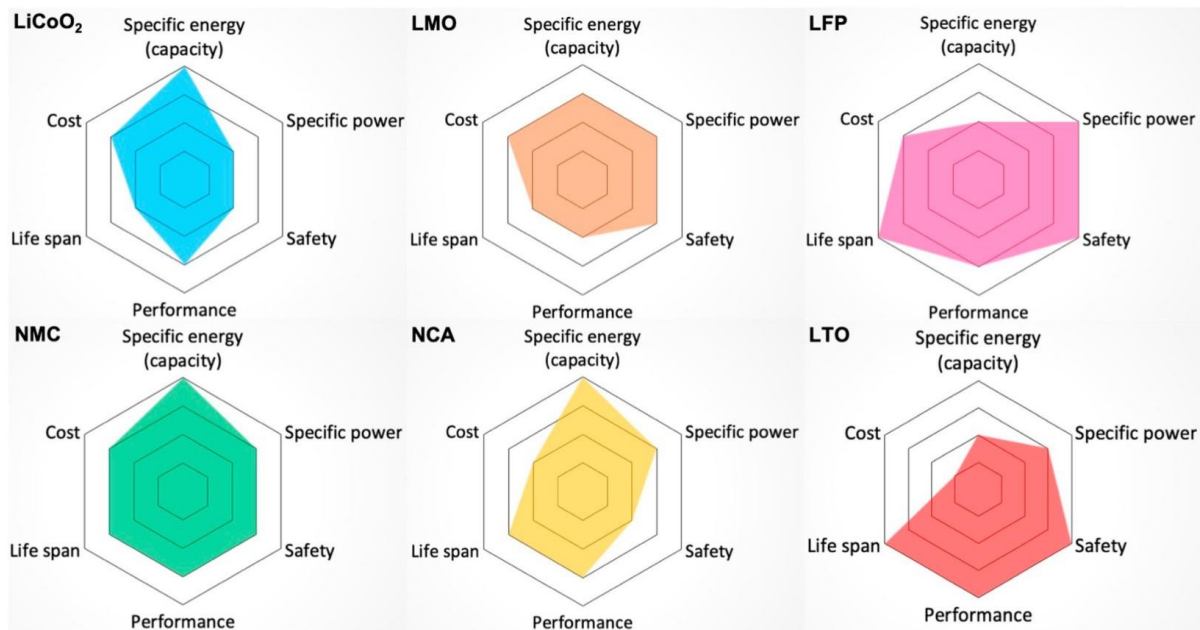


Figure 1.10: Types of Li-ion battery chemistries and their features[22].

Some of the widely used Li-ion battery types are Nickel Manganese Cobalt Oxide (NMC), Nickel Cobalt Aluminum Oxide (NCA), Manganese Oxide (LMO), and Iron Phosphate (LFP). Each battery type has its own perks and disadvantages and possesses its unique characteristics.

The NMC cell has a large energy density (275Wh/kg), and its voltage level is high (4.2V) but suffers from thermal degradation and portrays lower cycle life. NCA cell has better thermal stability however it suffers from lower power density. LMO cell has higher stability than NCA cell, but an average power and energy density limits their wider applications. On the other hand, LFP cell has the longest cycle life and is the most stable and safest chemistry of all. It doesn't suffer from internal heating and possesses a higher power density. However, lower energy density (150 Wh/kg) and voltage level (3.2V) are few negatives which could limit its application [23].

Even though many differences occur, LFP batteries are cheaper to produce making the end-product affordable. They are also long-lasting and have a lower risk of internal heating damage. The LFP cell's performance under different temperature gradient is exceptional and is known as the safest and the most stable chemistry of all due to the inclusion of Iron (Fe). Apart from that, the flat voltage curve provides a constant output power and can be charged fully to avoid without any capacity degradation [24].

1.1.7 Degradation of cell analyzed through EIS

Li-ion batteries do have safety issues and are often faced with different degradations over time. To address these issues, research must be focused on studying those degradation mechanisms and internal behaviour of Li-ion kinetics in order to improve their performance and efficiency.

Specifically, the rate at which chemical reactions inside the cell of a Li-ion battery occur is often influenced by internal resistances, composites, and other behavioral characteristics [25]. Kinetics or how fast a reaction occurs can show variations with external parameters including the environmental or ambient temperature, charging/discharging rates, and degradation after certain number of cycles [26].

Another aspect which can influence the kinetics as well as the performance of Li-ion cell are the internal impedances or resistances. Inside a cell, there are many kinds of electrochemical reactions happening before its formation, during charging and discharging, and even at rest. These reactions contribute to various kinds of impedances i.e., charge-transfer resistance, electrolyte/solution resistance, surface resistance, and interfacial resistance etc. These resistances/impedances can be studied using Electrochemical Impedance Spectroscopy (EIS). This

technique provides impedance analysis with respect to varying frequency which can highlight underlying mechanisms and behaviours of Li-ion cells [27].

Henceforth, this study combines the parameters which can have influence on the kinetics of Li-ion cells with EIS to study deeply how internal impedances and mechanisms change with kinetic parameters and how they influence the different reaction kinetics inside the Lithium-Ion cylindrical cells.

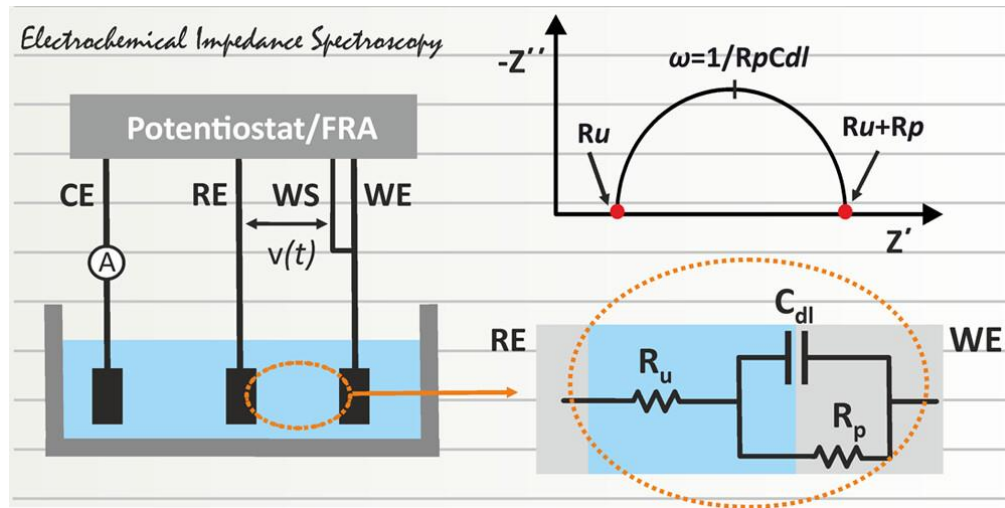


Figure 1.11: EIS and its valuable information extraction [28].

1.1.8 Effect of Temperature and C-rate on Degradation

The temperature in Li-ion cells plays a key role in its performance and as well as its cycle life. Many research areas focus on studying internal temperature changes and their effects on their performance as well as external temperature benefits. Some chemistries like NMC are highly affected by the higher temperatures while most of the cell types are affected by the lower temperatures near freezing point. Meanwhile, LFP cells show stable characteristics throughout their temperature range with few exceptions.

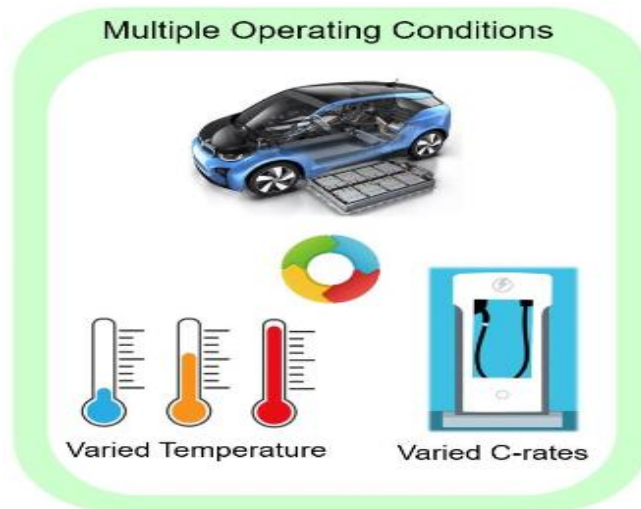


Figure 1.12: Effects of temperature and c-rates on Li-ion battery [29].

The charging/discharging rates or c-rates have a significant impact on battery life. All types of cell chemistries show degradation with increasing discharge rates with some showing fewer dependence like NCA and LFP while others are highly dependent like NMC. The impact of high discharge causes thermal runaway and breaks down the internal electrode's structure or diminishes the electrolyte of the cell. On the other hand, fast charging behaviour shows variable characteristics as it is a highly desirable factor in today's EV manufacturing, Due to widespread usage of EVs, there is a strong demand to reduce high discharging impacts and to make better use of fast charging to avoid long waiting hours. These are the highly researched area nowadays and demands a thorough study for better implementation of Li-ion batteries [30].

1.2 Problem Statement

The Li-ion batteries face various damages and degradation reactions which in turn causes thermal runaway, safety hazards, dendrite formation, particle cracking etc. These unwarranted reactions and their products are subjected to rigorous cycling conditions including c-rates, internal temperatures, and number of cycles. These reactions are also affected by ambient conditions like temperature, humidity, and pressure. Apart from the safety concerns, the decrement in capacity upon its cycling poses a certain hindrance to Li-ion battery implementation. Henceforth, there is a need of fundamental understanding for internal behavior of Li-ion cell with respect to the kinetics of various degradation mechanisms and what their products result in.

1.3 Research Hypothesis

This research study would successfully link the internal behavior changes with respect to the cyclic as well as the ambient environmental conditions with the impedance changes. After the proposed number of cycles, the cell would show capacity degradation and variable electrochemical behaviors. This will help in better understanding the underlying degradation behaviors, reaction kinetics, and their mechanisms. It will also serve as a useful dataset for further work on modelling those effects and to even predict the parametric related trends in the future.

1.4 Objective

The objectives of this study are to:

- To investigate the kinetic behavior of LFP (Lithium Iron Phosphate) cells at different c-rates and temperatures
- To analyse the performance of the cell after various number of charge/discharge cycles (0~100% SOC)
- To showcase the electrochemical impedance behavior at extreme ambient temperatures

1.5 Scope of the Study

This study involves the analysis of fast-charging behavior of the cells which is a major requirement of the latest Electric Vehicles' operation and their charging stations. The kinetic studies help in identifying various electrochemical reactions which can contribute towards building better and efficient BMS (Battery Management Systems), can help in grid-level batteries' implementation providing with more awareness and predictability of cell's internal behavior, and it can also help in creating forecasting/predicting models for further analysis.

Many of the current renewable energy storage systems utilize energy storage systems like Li-ion battery packs. Hence, this research study can make it affordable, applicable, and better aware of Li-ion battery backup in renewable energy systems like Solar, Wind, etc. Micro-grids running on hydel power can also utilize Li-ion batteries as the study reveals crucial performance

indicators for longer utilization of these batteries and along with variable load profiles with its high-discharge analysis.

1.6 Summary

This chapter introduces background information regarding current energy affairs and provides a renewable solution to tackle the problem. It further highlights the challenges of its implementation as renewable energy sources are intermittent and expensive. The implementation of Li-ion as a viable alternative to lead acid batteries is briefed upon and the various hazards it possesses are briefed upon. The chapter opens the discussion of why Li-ion batteries are important and what can be done to improve their implementation and application.

CHAPTER 2: LITERATURE REVIEW

2.1 Literature

The energy storage systems are one of the fundamental requirements to supply sustainable energy flow and to cater the demands of peak hours. The energy demand is increasing at a rapid pace of about 5% annually and hence, the target of International Renewable Energy Agency (IRENA) is to increase the proportion of renewable energy by 57% worldwide by 2030 [31]. However, renewable energy systems are dependent upon natural resources which are independent of human control, and they possess dynamical power supply. Therefore, they require an energy storage system which can store extra energy and can aid in reducing supply and demand gap during peak hours. There are many types of energy storage systems including electrochemical energy storage, thermal energy storage, thermochemical energy storage, flywheels, pumped -hydro, compressed-air storage, etc. [32]. However, for renewable energy systems, mainly battery storage systems are being used due to their moderately high power and energy capacity [33].

Batteries are one of the electrochemical energy storage systems which converts electrical energy into chemical energy while charging and does the opposite during discharging. The redox reaction inside a battery causes these conversions to take place [34]. The battery system consists of various components and each component plays a crucial role in storing and converting energy from one form to another.

There are mainly two types of batteries which are divided based on their chargeability. Primary cells are the cells which can't be recharged and are used till their electrodes experience total breakdown. Secondary cells are the cells which can recharged if they are fully discharged until the end of their life cycle [35]. An example of primary battery is Alkaline primary cell which has a unique structure to store electrochemical energy and lasts long without any recharge. An example of secondary battery is Nickel Cadmium secondary battery. The NiCd secondary cell has jelly-roll type shape and has a separator between its anodes and cathodes. This configuration allows for larger energy density to cope up with secondary battery's lesser energy yield in a single cycle as compared to primary battery or cell [36].

As discussed above in [33], the renewable energy systems utilize secondary battery systems as they are rechargeable and can last for many numbers of cycles, decreasing energy storage cost significantly. Hence why, the application of primary batteries and cells is limited and aren't feasible for renewable or electric vehicle storage systems. Therefore, secondary battery types will be discussed further for its suitability.

Secondary batteries possess the ability to reverse its electrochemical reactions upon supplying current to it. This leads them to have better power density, stability upon cycling, and longer usability [37]. There are various kinds of secondary batteries being manufactured in the market these days including Lead Acid, Nickel battery, Silver battery, Li-ion Battery, and Metal-Air Battery [35]. Lead-acid battery is one of the secondary batteries which consists of Lead-dioxide (PbO_2) cathode, Lead anode, and Sulfuric acid (H_2SO_4) electrolyte [38]. NiCd battery consists of nickel-hydroxide cathode, cadmium-plated anode, and potassium hydroxide electrolyte [35]. Li-ion battery consists of usually a graphite anode, lithium-based cathode, and lithium hexafluorophosphate salt (LiPF_6) electrolyte.

Lithium-ion battery is the most widely used batteries in the world today. However, with numerous advancements, Li-ion batteries have various types of electrodes and electrolytes being commercialized recently. However, their wider applicability is being hindered by the lack of understanding of their aging mechanisms and operating conditions.

One is a capacity loss where they are unable to provide requisite energy, and the second is power loss, where the battery is incapable of providing the required power [33]. Three primary parameters can be used to characterize a battery: functional capacity, state of charge (SOC), and state of health (SOH). For efficient usage battery, its capacity must be able which provide the required energy. These parameters degrade with time depending upon usage in any condition. The aging process of battery results in lowering the efficiency of systems. Different reasons for the degradation of a battery are corrosion of electrodes, loss of electrolyte, and active mass detachment. These factors cause internal damage to batteries and result in both capacity and power loss [34].

In general, battery performance depends on operating conditions that include operating temperature and humidity, Depth of discharge, charging and discharging current and storage

conditions. In another study, authors assembled four cells of 25Ah, were cycled at low and high temperature. All four cells were cycled at current rate $C/12$ and $C/3$. It was determined that a quicker charging rate at $C/3$ at higher temperatures causes a battery to degrade rapidly.

Temperature is one of the most influential factors in determining battery performance. Optimum temperature set for battery performance is $25\text{ }^{\circ}\text{C}$. At higher temperature, battery capacity increases, but the degradation rate also increases [39]. In a study in [40], authors have determined bad recharge, time since last full charge to be also affecting the battery's performance. Additionally, incremental capacity analysis was used to examine the performance of lithium-ion batteries at $25\text{ }^{\circ}\text{C}$ and $60\text{ }^{\circ}\text{C}$. It was found that the loss of active ingredients or the depletion of the lithium stock due to electrochemical milling is what causes the capacity to degrade at higher temperatures [41]. Similarly, in studies[42], [43], the cycle life of a battery is affected by the depth-of-discharge, discharge/discharge rate and temperature. Further, to evaluate the performance of lithium-ion battery at lower temperature, authors in study[44], at three different temperatures, cells were cycled., (room temp, $0\text{ }^{\circ}\text{C}$, and $-18\text{ }^{\circ}\text{C}$), under consideration of load in simulation of an electric vehicle. the evaluation of a cell's electrochemistry before and after cycling. In the cell that cycled at $0\text{ }^{\circ}\text{C}$, there were also some signs of lithium plating on the surface of the graphite electrode, although it was much less severe than in the cell that cycled at $-18\text{ }^{\circ}\text{C}$. In a different investigation, three factors were examined on cells: temperature ($-30\text{ }^{\circ}\text{C}$ to $60\text{ }^{\circ}\text{C}$), depth of discharge (90 % to 10 %), and discharging rate ($C/2$ - 10 C). The capacity loss was highly influenced by time and temperature at the low C-rates, although the DOD impact was less significant, according to experimental data. The charge/discharge rate effects were most pronounced at high C-rates. Capacity characterization and EIS techniques were used to evaluate the condition of the battery in this study[45]. In a study [46], authors used Li-ion cells to examine the combined influence of driving and vehicle to grid usage on a life cycle of the cell. The experiments showed that battery degradation is less than 5 % after being used over hundreds of driving days. In a study by authors in [47], Li-ion battery of 900 mAh was tested to determine the effect on performance and evaluation of battery. It was determined that while the discharge circumstances have a minimal impact on cycle life, the charge conditions have a significant impact. High charge rates over the IC rate are a further risk factor, however unlike with other rechargeable batteries, the DOD decrease does not extend cycle life.

Apart from experimental methods, various models have been designed to better understand the cycling effect of battery, along with degradation [48]. These battery models can be used to predict its behaviour under different operating conditions [48], [49]. Three main kinds of model are present in the literature. Electrochemical models that simulate the behaviour of physiochemical properties of batteries. Variables in this model include mass transport, thermodynamic, electrical, mechanical properties [50]. Analytical Models which are based on interpolation and extrapolation obtained from data acquired from manufacturers. They have reduced complexity when compared electrochemical models [51]. The third type is based on an electrical circuit model. It includes voltage, resistors, capacitors, and inductors [52]. In study [53], the authors modelled complex, nonlinear behaviour of electrochemical using equivalent electric networks. It was concluded that although these networks contain elements that are nonlinear and depend on battery state-of-charge and electrolyte temperature, they are very useful tools for understanding internal battery electrochemical reactions in terms of electric quantities. In literature [54], the authors proposed a dynamic model of Li-ion battery considering the effect of temperature and capacity fading. Simulation result showed that the model can truly reflect the dynamic characteristics of battery and it can be directly used in different simulation models. Similarly, in another study, authors investigated modelling and parameter identification of Li-ion battery to be used in the Simulink environment. The comparison showed that simulation and hardware tests show a high degree of accuracy [55].

Using an equivalent model for evaluating the performance of battery had been used in many studies. The main type of electric models that can be used to simulate the behaviour of a battery is a simple battery model, Thevenin model, Schiffer model, first order, second and third order model. These models are described in detail in [56]. In another study, using the same model technique, the authors applied state of health monitoring to develop a method for evaluating the performance of LIB. For this model was designed using the 2RC branch of equivalent circuit modelling including thermal module and aging function. The aging function was supported by experimental measurements. However, it was concluded that for the accurate working of a model, the experimental data should be more accurate, or the model would give invalidated results [57].

Lee et al. [58] utilized GITT, PITT, EIS, and CV to evaluate two critical parameters: diffusion coefficient and exchange current density, employed them to determine the

electrochemical characteristics of the NMC cell and their application on an electrochemical model (based on Newman's model) shown in Figure 2.1. They observed that without any fitting done to match the actual electrochemical behaviours, actual voltage-capacity profiles were reported by the model adopting the parameters measured by PITT and EIS. To evaluate the performance of batteries during and after cycling, various techniques are used, e.g., EIS and XRD [39]. EIS, electrochemical impedance spectroscopy, is an in-situ technique to understand the impedance behaviour of a battery. It is based on the frequency response of the sinusoidal signal. The impedance spectrum battery generally consists of an inductive tail at high frequency, intercept with Zre axis (HFR), represents ohmic resistance. Then there are semicircular arcs at mid-frequency attributed to SEI layer and charge transfer resistance. The third region is a tangential line that represents diffusion at low frequency. EIS can be used to analyze the aging of the battery due to various reason [59].

2.2 Summary

This chapter describes in detail, different studies that have been carried out for performance evaluation of batteries. Main technologies of batteries are Lead acid and lithium batteries. Lithium-ion battery currently holds the majority of market share, due to its high energy and long cyclability. Parameters to characterize any battery are remaining capacity, SOC, and SOH. The main reason for degradation of batteries over cycling is linked to discharge current, charge/discharge cycling, and temperature. Studies on performance evaluation of batteries have used either experimental method or software methods. In EIS, impedance values of batteries are analyzed throughout cycling, to determine the degradation rate, under given operating conditions.

CHAPTER 3: Review of Experimental & Characterization Work

In this chapter, a thorough review of the experiments ran, and the characterization techniques used are discussed. There were two types of testing which were carried out, one was on Battery Analyzer for charge/discharge, and the other was on Electrochemical Workstation for electrochemical impedance spectroscopy. For these tests, a thermal chamber was also customized for temperature-based readings along with a digital data-logger and microcontroller. These topics are discussed below to give an insightful review on experiments and characterization work of this study.

3.1 Battery Analyzer

The Battery Analyzer is a device which is used for charging/discharging of the cells of various kinds like coin cells, cylindrical cells, pouch cells, and various kinds of batteries shown in figure 3.1. The device contains a voltage rating usually 5V, which sets the maximum limit for the cell under study as their voltage can't exceed that limit. Another limitation is current rating which sets the limit of charging and discharging current. As a result, the cells undergoing test can't be charged or discharged above the rated current of the device.

The 8-channel battery analyzers also provide customized current and voltage safety to the cells under study. The upper cut-off voltage safety of the cells was set at 4.0V while the lower cut-off voltage safety was set at 2.0V as specified by the manufacturers during this study.

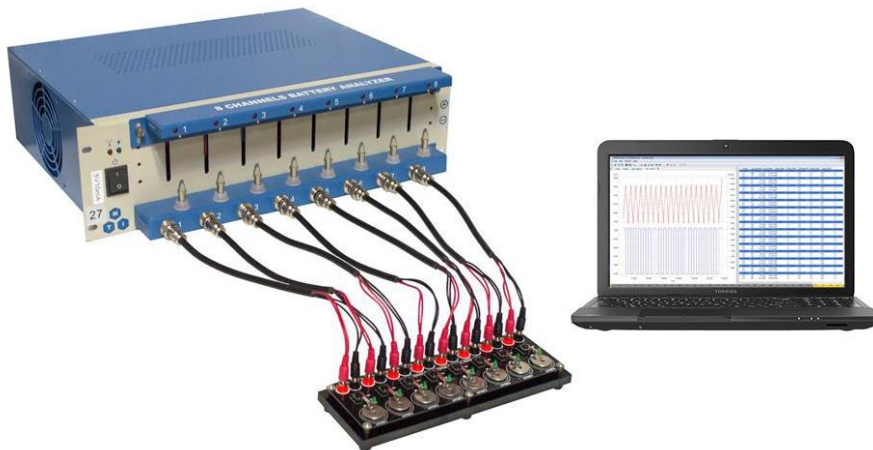


Figure 3.1: Battery Analyzer setup with its connections [60].

The battery analyser consists of various types of operating modes which includes constant current charge, constant voltage charge, constant current and voltage charge, and constant current discharge. These modes can be used to measure the remaining capacity and cycle life of batteries. This information is useful in newly built electrodes, performance testing of batteries, and for lab-scale battery designing. The built-in software in these devices generates real-time as well as post-experimental graphs. These include voltage time graph, current time graph, capacity voltage graph, cycled charge/discharge graph, cycled capacity graphs etc.

3.1.1 Testing Conditions

There are various conditions of testing a cell, but they all need to go through some form of charging or discharging for viable testing. There are three forms of charging method while a single form of discharging method is commonly used. The methods are discussed below:

3.1.1.1 Constant Current Charging

In Constant Current (CC) Charging, the battery or the cell is charged at a specified or a given current rate until the battery reaches its maximum or specified potential. Throughout this charging, the current remains almost at a constant value while the voltage increases till its maximum value [61], [62]. For the safety purposes and to avoid the build-up of gasses inside the cell, it is recommended that the charging current should be limited to about 25~30% of the capacity of the cell while the voltage limit shouldn't exceed 100% SOC of the battery [63] [5].

3.1.1.2 Constant Voltage Charging

In Constant Voltage (CV) Charging method, the voltage of the power source is kept at a constant voltage and the battery, or the cell is charged upon this condition. The current in this situation is proportional to the internal resistance of the battery according to Ohm's law, however, it's advisable to put a safety limit to the current so it may not exceed battery's charging safety limit. Initially, the charging current is at the highest but as the voltage of the battery increases, the potential difference between the source and the battery decreases, hence, the current also decreases. Therefore, in CV charging method, the voltage remains constant while current decreases until the current is at its minimal value or zero as an ideal case [61], [63].

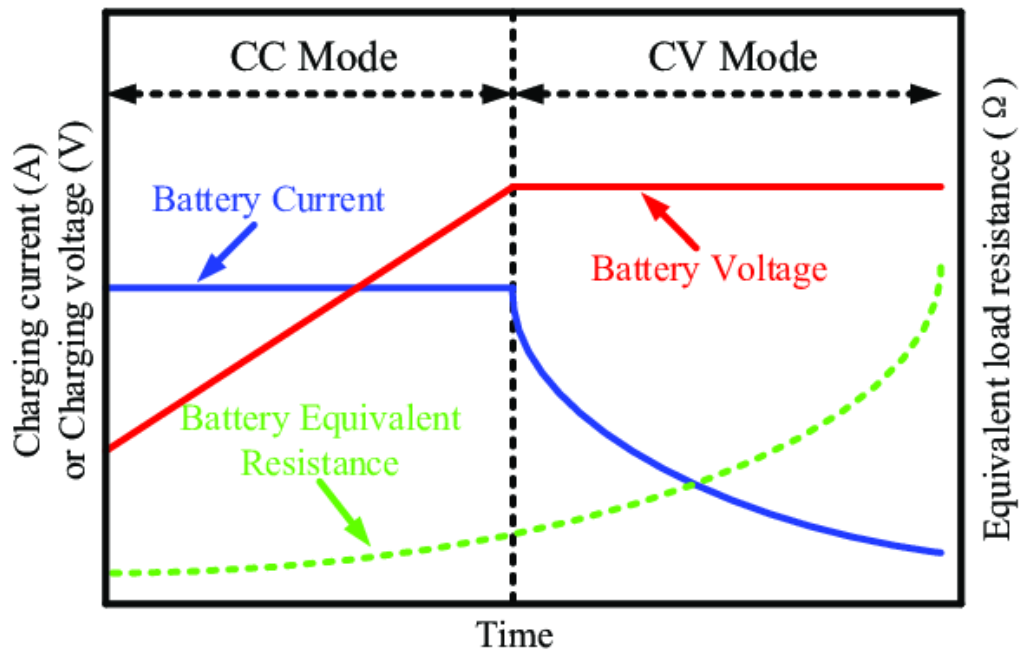


Figure 3.2: Various charging methods shown including Constant Current & Constant Voltage Charging [64]

3.1.1.3 Constant Current & Constant Voltage (CC-CV) Charge

In the Constant Current and Constant Voltage (CC-CV) charging method, the battery analyser or the source first charges the cell or the battery at a constant current to increase the voltage level to the desired value, usually till 100% SOC. Then, once the desired voltage is reached, the charging mode automatically shifts to constant voltage mode in which the current is slowly

decreased while maintaining the voltage constant. As soon as the current reaches the cut-off point, the charging completes. As shown in figure 3.2, during CC mode, the current remains same but as soon the CV mode starts, it starts decreasing. As for the voltage, it starts increasing in CC mode until its maximum potential, then, during the CV mode, it remains stable and nearly same throughout until the end of charging.

ID	Step name	StepTime(hh:mm:ss.ms)	Rate(C)	Volt(V)	Cur(mA)	Cap (Ah)	Stop Rate(C)	Stop Cur(mA)
1	Rest	01:00:00:000						
2	CC_Chg			4.0000	2.0			
3	CV_Chg			4.0000	2.0			0.2
4	Rest	01:00:00:000						
5	CC_Dchg			1.0000	2.0			
6	CV_Dchg			1.0000	2.0			0.2
7	Rest	01:00:00:000						
8	DCCV_Chg			4.0000	2.0			0.2

Figure 3.3: The CC-CV charging settings shown on a battery analyzer [7]

Figure 3.3 shows an example of CC-CV charging settings of a battery analyzer where the user must set the charging constant current and the maximum voltage and, for CV mode, the stopping current is required in order to ensure the end of charging since the voltage would remain same e.g., 4V as shown in the figure. This method is usually used for lead acid and, nowadays, trending Li-ion batteries. The charging speed can be set from the CC mode by selecting a higher current and the full capacity can be utilized from the CV mode by selecting a lower cut-off current. Therefore, the CC-CV method is much more efficient as it combines the advantages of both methods[65].

3.2 Electrochemical Impedance Spectroscopy (EIS)

Electrochemical Impedance Spectroscopy is a characterization technique that is used to investigate and study the behaviors of various electrochemical systems for their kinetics, corrosion, and physio-chemical processes. It is extensively used in energy storage and conversion systems, chemical and bio-sensing systems, and semiconductor systems. EIS technique employs an ac signal consisting of multiple frequencies to an electrochemical system and analyses the output response of that system to that ac signal. This analysis reveals valuable information of the system

under study as it incorporates time-varying processes and turns them into frequency-dependent processes. Hence, the response or the impedance spectrum simplifies the complex behavior of an electrochemical system [66].

3.2.1 Working

Electrochemical Impedance Spectroscopy (EIS) works on the basis of applied ac sinusoidal signal. The input signal can be of two types: ac voltage (potentiostat) or ac current (galvanostat). The response or the output is opposite in nature i.e., for voltage, it's current and vice versa. However, the output signal is dependent upon internal impedance of the system which are characterized by resistive, capacitive, and inductive behavior. The output signal is usually phase shifted in its frequency response and has varying amplitude as well. The response then produces an impedance spectrum as EIS works as a transfer function for time-invariant functions or systems. The impedance response is further analyzed and is presented in the graphical form, usually in Nyquist and/or Bode plots.

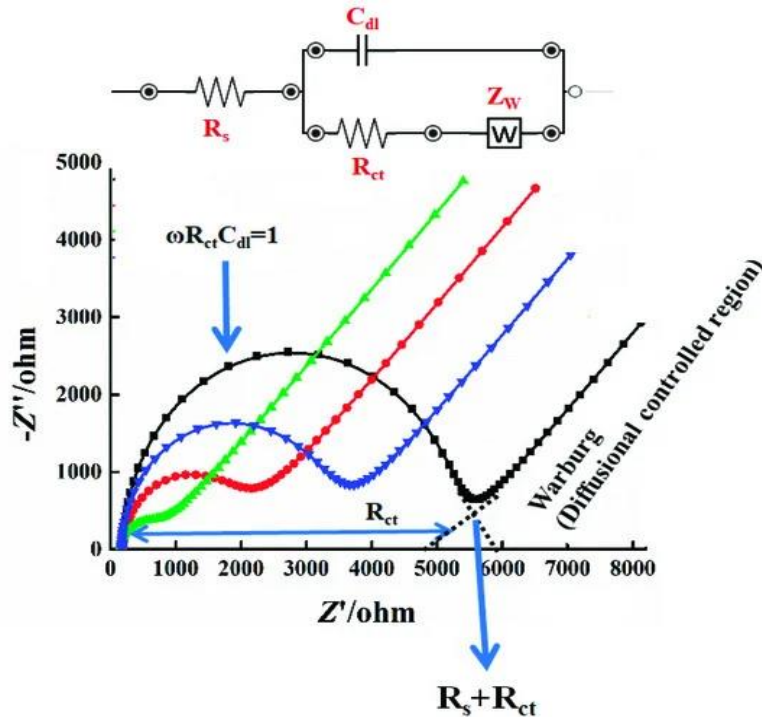


Figure 3.4: Nyquist plot along with equivalent circuit model derived from EIS test [67]

An EIS test simplifies and makes it easier to understand various underlying phenomena inside an electrochemical system as there are different physio-chemical reactions taking place

and it's complex to decipher them apart. Since every process has a different time constant or ' τ ', the time it takes for a process to complete, it gets difficult to set them apart. The EIS technique deals with them by changing them into frequency domain and as a result, individual process can be determined based on their operating frequency i.e., quick processes show higher frequencies while slow processes show low frequency. From figure 3.4, an example of Nyquist graphs is given along with its equivalent circuit model. As it can be seen from the graph, the charge-transfer process, the electrolyte resistance, the double-layer capacitance, and diffusion process can easily be deciphered based on their frequency. The equivalent circuit model simulates the result and provides an equivalent electrical model for better analysis of the results. It can be used further for predictive modelling or for any other type of applications.

3.3 Thermally Insulated Chamber or Environmental Chamber

For temperature-based testing, a thermally insulated chamber was designed for the cells under study. This environmental chamber provided a heated ambient environment and was specifically designed to not leak any heat and make the experiment more accurate and repeatable. The chamber was temperature controlled and was fully automated for its reliability and had proven to be resilient to rigorous testing as well. Its major components are discussed below:

3.3.1 PTC Element

A PTC element or positive temperature coefficient is a heating device which gives off heat due to electrical current. The device consists of a thermistor inside which has a tendency to increase its resistance upon increase in the temperature. The current flowing inside causes the resistance to increase and once the resistance increases, the current drops and helps to regulate the temperature of the device. This self-regulation of the device helps in maintaining its temperature and in providing a constant-temperature heat source[68].

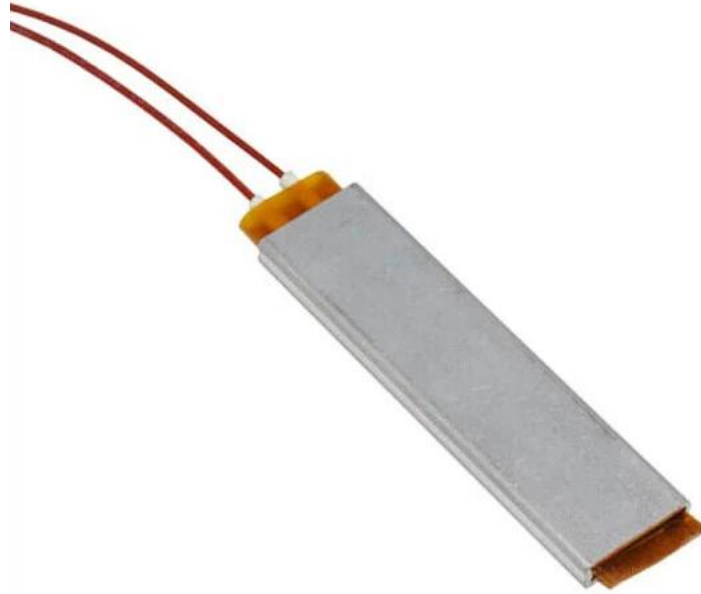


Figure 3.5: A PTC device with aluminum body for heat uniformity [69].

Figure 3.5 shows a PTC with aluminum body for even heat distribution. This PTC operates on AC voltages and can reach temperature up to 250°C. This type of PTC is mainly used in heaters, hair dryers, and vehicle heating.

3.3.2 W1209 Temperature Controller

The W1209 temperature controller is an automatic thermostat device which controls the temperature of an environment using a microcontroller and a sensor. The microcontroller is already programmed and doesn't require any further programming. The device consists of various setting parameters including application type (heater or cooler), temperature range, and safety limits[70].

In it, a specific sensor known as NTC is used which is further discussed below. The W1209 module works by connecting or disconnecting a heating or cooling source through energizing an in-built relay. Once the desired temperature is reached, the microcontroller senses the temperature and triggers the relay accordingly.

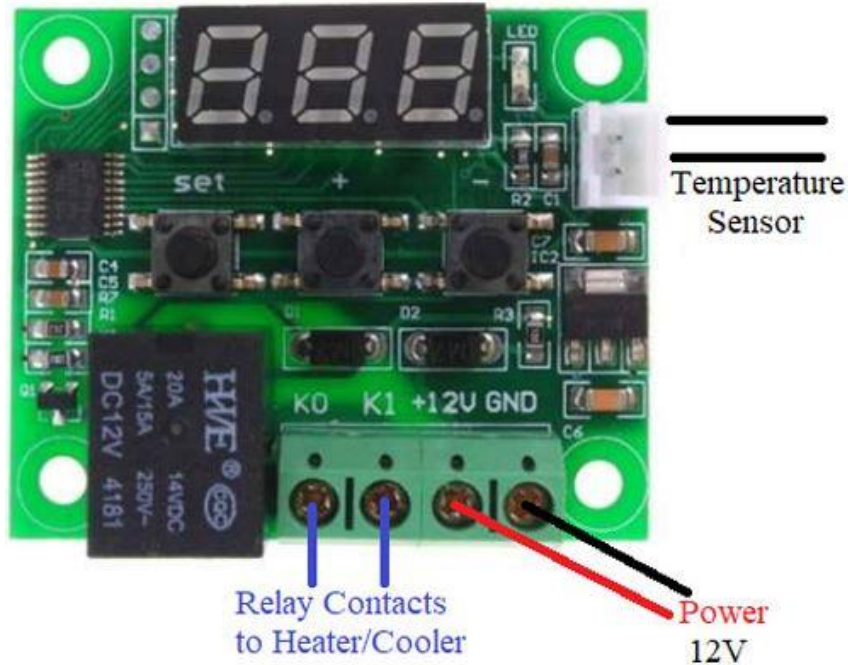


Figure 3.6: A W1209 temperature controller with its components labelling [71].

The figure (3.6) displays a W1209 controller with its parts being labelled. From the figure, the temperature display is visible while the inputs are marked accordingly. The temperature sensor wiring is shown where the NTC temperature is connected. The controller is run by a 12V DC source while the heater/cooler can either be of AC type or DC type. This controller can control temperature in the range of -50°C to 110°C and can operate the heating/cooling source of up to 10A.

3.3.3 NTC Sensor

As discussed above, the W1209 temperature controller uses an NTC sensor for temperature sensing. An NTC is a negative temperature coefficient resistor or better known as thermistor. This resistor has semiconductor materials which, upon conducting electrical current, heats up but their resistivity decreases. This is why they are known for their negative temperature coefficient because as temperature increases, their resistance decreases and vice versa [72]. The NTC temperature sensors are used for applications involving common heating sources as the NTC doesn't perform well on temperatures above 300°C . The sensor shown in figure 3.7 is specifically used in W1209

controller as it involves two input pins with a long chord connected to the NTC sensor. This type of sensor is suitable for sensing temperature below 100°C.



Figure 3.7: An NTC sensor used in W1209 temperature controller [73].

3.3.4 Monitoring System

The experiments being tested were monitored for their temperature variations using a k-type thermocouple and data logger. The k-type thermocouple was necessary for accurate sensing of the ambient temperature while the data logger monitors and records the data continuously for real-time as well as for future references.

3.3.5 k-type Thermocouple

A thermocouple is a sensor which comprises of two unmatched alloy that react to the heat differently. One is made up of Alumel material while the other is Chromel. These two alloys are twisted together to form a junction enabling the formation of a thermocouple with two legs. The Chromel is made up of nickel and chromium while the Alumel is made from nickel, aluminium, and manganese [74].

The k-type thermocouple works when the sensor is touched to the heated surface or experiences heated air or surrounding and since the metals have varying materialistic properties,

the temperature creates different resistances between them. This builds up the voltages and hence, the current is generated based on the temperature.



Figure 3.8: k-type Thermocouple with its two legs [75].

3.3.6 Data Logger

A digital data logger is an electronic device that is used to record and store data over time. The device typically has one or more sensors that measure a physical parameter, such as temperature, humidity, pressure, or light, and a microprocessor that converts the analog signal into digital data and stores it in memory. The data can then be retrieved from the device and analysed using software. Digital data loggers are widely used in a variety of applications, including scientific research, industrial process control, environmental monitoring, and building automation. They offer several advantages over traditional data logging methods, such as paper records or manual data entry, including:

- **Accuracy:** Digital data loggers typically have high accuracy and resolution, allowing for precise measurements of physical parameters over time.
- **Convenience:** Data loggers can be programmed to record data automatically at regular intervals, eliminating the need for manual data collection and reducing the risk of human error.

- **Portability:** Digital data loggers are often small and lightweight, making them easy to transport and deploy in remote or hard-to-reach locations.
- **Storage capacity:** Many digital data loggers have large memory capacities, allowing for long-term data logging and storage.
- **Real-time monitoring:** Some data loggers can transmit data wirelessly in real-time, allowing for remote monitoring and analysis.



Figure 3.9: Digital Data Logger

Some common features of digital data loggers include programmable recording intervals, alarm functions, battery-powered operation, and the ability to connect to a computer or other device for data transfer and analysis.

3.4 Summary

This section describes in detail the experimentation and characterization methods with a focus on the implementation details. The chapter discusses the charging discharging method and electrochemical techniques including EIS their mathematical explanation, the factors considered in implementation of these techniques and the comparison of the results obtained for different calculations.

CHAPTER 4: Experimental Methodology

In this chapter, a review of experimental setup along with characterization techniques is discussed. Firstly, the tested cells are discussed followed by an introduction of the electrochemical characterization techniques and lastly, the testing protocols are briefed upon.

4.1 Tested Cells

In this study, LiFePO₄ (LFP) commercial cells of 18650 model were subjected to various testings. The cells were bought from Akkuteile company (Model # IFR 18650, 1500 mAh). The cell's specifications are summarized in Table 4.1.

Table 4.1: Lithium-ion Iron Phosphate (LFP) commercial cell of 18650 model with their specifications provided by Akkuteile manufacturers.

Nominal Capacity (mAh)	Nominal Voltage (V)	Charging End Voltage (V)	Max. Discharging Current (A)	Max. Temperature (°C)	Size: Diameter, Height (mm)	Nominal Weight (g)
1500	3.2	3.6 ± 0.5	4.5/3C	60	18.0 ± 0.3, 66.1 ± 0.5	41 ± 1

4.2 Battery Analyzer, Electrochemical Impedance Spectroscopy (EIS), & Thermal

Chamber setup:

Cells were cycled in three different Battery Analysers having various limits: Battery Analyzer 1 (5 V, 30 A), Battery Analyzer 2 (5 V, 3 A), and Landt Battery Analyzer (5 V, 2 A). These 8-channel battery analysers provided current and voltage safety to the cells under study. The upper cut-off voltage safety of the cells was set at 4.0 V while the lower cut-off voltage safety was set at 2.0 V as specified by the manufacturers. The Electrochemical Impedance Spectroscopy (EIS) was performed on the Electrochemical Workstation of model CHI 660e. The EIS tests were performed using Galvanostatic technique with frequency range from 1 kHz to 0.01 Hz. The cells were connected in 4-electrode configuration with cell's cathode (positive side) connected to the working

and sensitive probe while anode (negative side) was connected to the reference and counter electrode throughout the experiment. [76]

The self-made thermal chamber was made from AC Heating element made up of PTC element (220 ~ 240 V, 100 watts) along with W1209 (temperature-controller) which was fitted with NTC temperature sensor and ran on 12 V-DC charger. The body of the thermal chamber was made from U-PVC with acrylic covers on top and bottom. Aluminium foil was used for even distribution of temperature throughout the chamber while for insulation purposes, glass wool sheet was wrapped around to avoid heat loss. Before any testing, the chamber was operated for ~1 hour until it achieved the desired temperature and then the temperature controller automatically controlled the temperature throughout the experiment. The W1209 microcontroller was programmed at a safety limit of 60 °C in order to avoid any thermal runaway of the cells. For the monitoring and recording of the temperature, a k-type thermocouple was used with ExTech's Datalogger TM500. [77]

4.3 Cyclic Protocols:

Firstly, the cells were tested on Electrochemical workstation for EIS response before cycling, or at '0th cycle'. Then, the cells were discharged according to their specific discharge-rate which were assigned to them during their cycling, till 2.2 V or 0 % SOC (State of Charge). The charging protocol used was CC-CV (Constant Current, Constant Voltage) mode while for discharging, it was CCD (Constant Current Discharge) [78].

Secondly, after these initial setups, the cells were allotted same charging/discharging rates (c-rates) which varied from 0.5 C (750 mA) to 2.5 C (3,750 mA) keeping in mind the 3C safety limit set by the manufacturer. The c-rates were increased by 0.5 C (0.5 C, 1 C, 1.5 C, 2 C, & 2.5 C) to thoroughly understand the internal behaviour as well as the performance of the cells. The cyclic protocol begins with charging at CC-CV mode till ~ 3.65 V (100 % SOC) and discharging at CCD mode till 2.2V (0 % SOC) with 5 ~10 minutes Rest time in between depending on the intensity of the c-rates. The cyclic testings were performed at room temperature (20 ~ 30 °C) as well as on extreme temperature (50 ~ 55 °C) by placing the cells inside the self-made thermally

insulated chamber, in order to study the effects of temperature while remaining in limits with manufacturer's assigned temperature (60 °C).

Thirdly, the Electrochemical Impedance Spectroscopy (EIS) was performed to investigate the charge-transfer resistance (R_{ct}) and other electrochemical behaviour of the cell. EIS testing was carried out after the 1st cycle, followed by the 100th cycle and finally at the 400th cycle by the end of the testing protocols. These tests were performed at room temperature for the cells cycled at room temperature while for the cells cycled at high temperature, the testing was also carried out at those temperature inside the self-made environmental chamber (Figure 4.1).

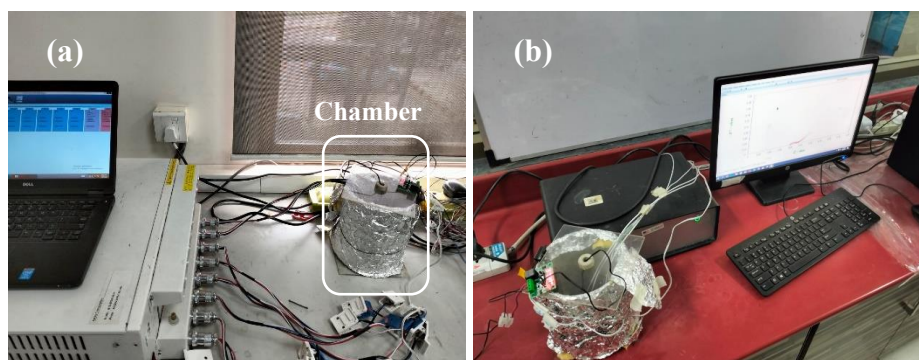


Figure 4.1: self-made environmental chamber to perform all experiment at 55 °C.

4.4 Summary

This section describes in depth the experimentation conducted as part of the research process. The fabrication of the coin cell is described in detail along with the techniques and instruments used and is thoroughly demonstrated in this chapter. At the end the derivation for the electrochemical testing technique is established methodically, and the testing parameters, are described in detail.

CHAPTER 5: Results and Discussion:

Electrochemical Impedance Spectroscopy (EIS) is a vital tool in determining the kinetic effects of any electrochemical system. The electrochemical testing of the cells which went through various conditions of charging-discharging rates, temperatures, and state of charges (SOCs) display variable characters and behaviors.

5.1 EIS study before cycling or 0th cycle

The commercial LFP cells were first tested without cycling or at as-prepared condition in order to figure out initial behavior of the cells. This will help in distinguishing and deciphering starting conditions from the experimented cells.

In Figure 5.1, the LFP cell's internal behavior without cycling or referred to as '0th Cycle' is displayed. Figure 5.1 (a) and (b) makes a clear comparison on the effects of temperature on the cell's internal performance. The series resistance, also known as solution or electrolyte resistance, ' R_s ', increases from 65.1 m Ω at room temperature to about 79 m Ω at elevated temperature of 55 °C. The charge-transfer resistance or ' R_{ct} ' is the resistance faced during ion-electron interaction on electrode-electrolyte interface. The exchange of charges during this interaction contributes towards R_{ct} . At room temperatures, the LFP cell faced a higher resistance of 8.64 m Ω as compared to 5.7 m Ω at 55 °C. This could mean that increase in temperature results in additional charge transfers or it assists in improving transfer routes by increasing diffusional paths.

The experimental data was fitted with equivalent circuit consisting of series resistance with an RC circuit and a Warburg element 'W' in the loop. The equivalent circuit in Figure 5.1 (b) shows two RC circuits with one having an ideal capacitor ' C_{dl} ' while the other is fitted with non-ideal capacitor or constant-phase element, 'CPE'. The first loop or RC circuit is due to charge-transfer resistance and double-layer capacitance while the second loop is caused by SEI formation. However, at room temperature, the absence of CPE or capacitive component indicates inactivity of electrode with electrolyte while at high temperature, it indicates minute faradaic reaction due to raised temperatures.

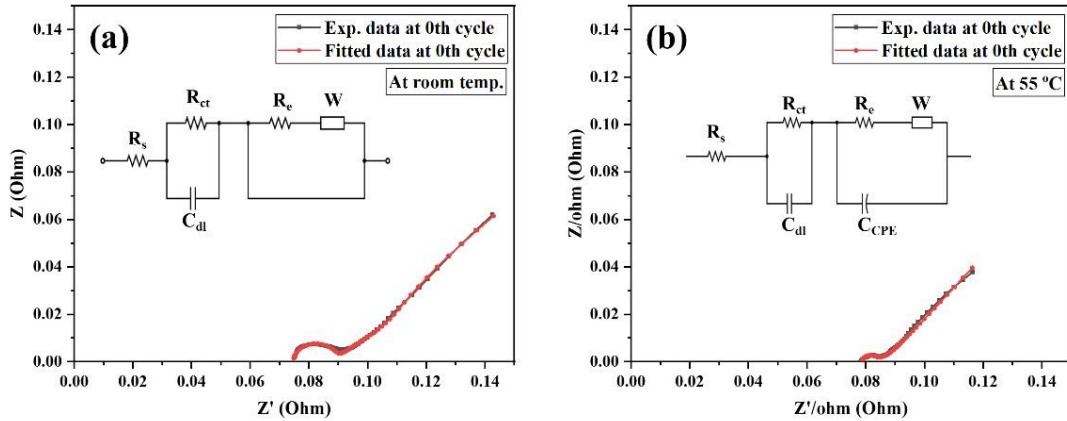


Figure 5.1: EIS testing before cycling at **a)** room temperature and **b)** 55 °C.

5.2 EIS testing after 1st cycle

The electrochemical impedance spectroscopy (EIS) was carried out after the first cycle of the cells to better understand the cell's behavior upon its activation. The results obtained would be beneficial for comparative study with cyclic data as it provides a sketch for initial conditions.

Figure 5.2 (a) shows a Nyquist plot of cells charged-discharged at room temperature and at various c-rates for a single cycle. The cells under study went through symmetrical charging and discharging at different rates. The c-rates were chosen based on an interval of 0.5 C and were kept below the safety limit of 3 C.

In the Figure 5.2 (b), the EIS of the cells tested with same exact conditions but at an elevated temperature of 55 °C is shown. The cycling was done in a customized thermal chamber made specifically for this study. The cells were first placed in a thermal chamber for an hour and then the tests were carried out. This provided an ambient environment with elevated temperature in order to mirror a heated real-life condition and to check the performance of the cells. Figures 5.2 (c), (d) & (e) show equivalent circuits obtained for the tests carried out at different c-rates and at 55 °C. The cells cycled at 0.5 C, 1 C, and 1.5 C show similar behavior in their Nyquist plots as it possesses two semicircles in the high frequency range and hence, are represented by similar equivalent circuit displayed in Figure 5.2 (c). The plots of the cells cycled at 2 C and 2.5 C are represented by Figure 5.2 (d) and (e), respectively. In an extensive work by Bing-Ang Mei *et al.*

[79], they demonstrated that there are many factors contributing towards the emergence of multiple semicircles in an electric double-layer capacitor (EDLC) electrode. Usually, the range of frequency in which they appear clarifies their reason for appearance. The high-frequency semicircle is commonly contributed by the electrode and current collector interfaces while the semicircles in the middle or lower side of the frequency are designated to electrode-electrolyte interfaces or to ionic diffusions near the electrode surfaces. Hence, the semicircles appearing in Figure 5.2 (d) and (e) can be said to appear due to the formations of different and new interfaces between the electrode/electrolyte. The fast charging/discharging at 2 and 2.5 C can also be the likely cause of disturbances and movements of ions near the electrode surface and hence, the new cell undergoes small perturbations in the form of small RC equivalent time-constants [80].

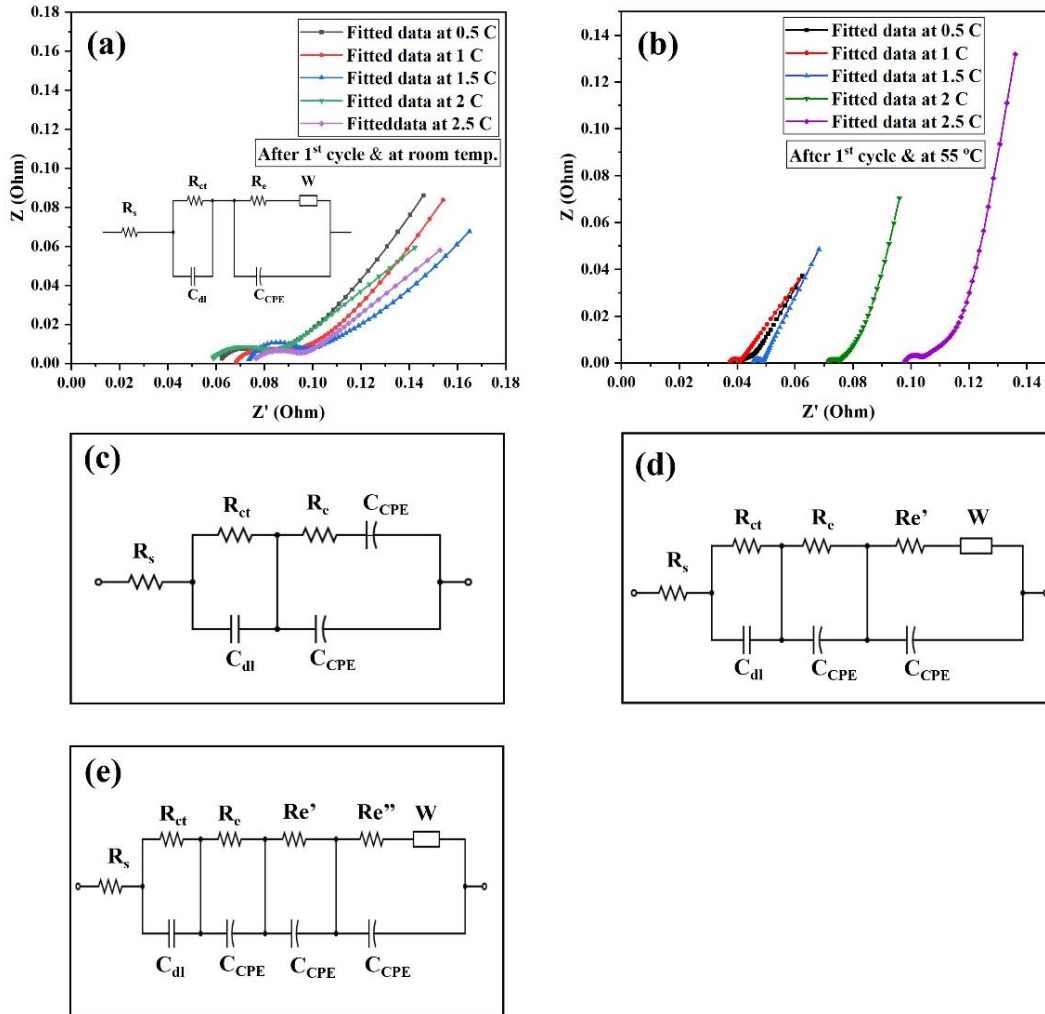


Figure 5.2: EIS testing after 1st cycle at **a)** room temp. **b)** 55 °C temperature. Equivalent circuits are shown for cells cycled at 55 °C temp. at **c)** 0.5 C to 1.5 C **d)** 2 C **e)** 2.5 C.

5.3 EIS testing after 100th cycle

The cycling of the cells was carried out till 400 cycles; however, an interval of testing was done at 100th cycle. Each cell was tested at different c-rates as mentioned previously in order to find the wide range of behaviors of the cell.

Figure 5.3 (a) & (b) represents a vital comparison of room temperature testing and at 55 °C temperature testing of the cells, respectively. The LFP cells, in the study done by Yulia Preger *et al.* [81], the cells underwent elevated temperature testing. They found out that LFP cells show

degradation upon increasing the ambient temperature of their environment. In a study published by Waldmann *et al.* in [82], it revealed that commonly, below a certain temperature, the Li^+ plating phenomena causes the degradation of the cells and above that temperature, the formation of SEI layer is what causes the degradation.

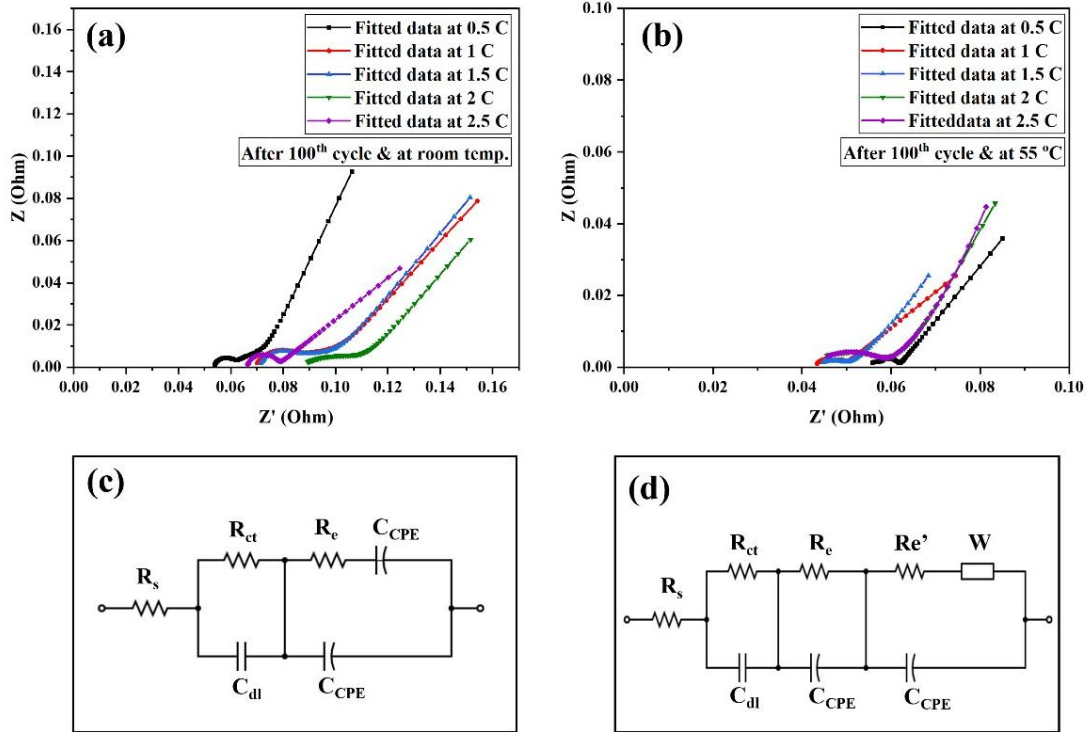


Figure 5.3: EIS comparison of cell cycled for 100 cycles at **a)** room temp. **b)** 55 °C temp. **c)** Equivalent circuit obtained for room temp. study **d)** Equivalent circuit obtained for 55 °C temp.

Figure 5.3 show that the cells under room temperature show an increase in their solution resistance, R_s , and as well as in their charge-transfer resistance, R_{ct} , upon increasing the c-rates. However, at particular 2.5 C rate, the R_{ct} decreases significantly as shown in Table 5.1 below. This decrement in resistance could show better performance of the cell at high c-rate of 2.5 C as fast charging/discharging caused more successful charge transfer events. However, it could also show possibility of potential dendrite formations causing better and faster charge transfer events but could lead to earlier degradation of the cell [83].

In Figure 5.3 (b), the high temperature testing after 100 cycles demonstrates various behaviors on different rates. The lack of c-rate dependency of R_{ct} show that the elevated temperature has caused internal disturbances in the cells under study. However, these temporal changes come under nominal behaviors as they tend to subside after the cell's internal impedance reaches equilibrium conditions. The equivalent circuit obtained from the Nyquist plot also correlates with this situation as there is an increase in RC circuits. The constant-phase element (CPE) in the circuit forming two RC loops show ionic movement hindrances [84], [85] causing buildup of charges however, the Warburg element in the lower frequency indicates smoother diffusion of these charges inside the electrode. Therefore, even though at some c-rates the charge-transfer resistance at elevated temperature is lower, some are showing larger resistance which could be due to these hindrances in the movements of ionic species from the bulk electrolyte towards the electrode's surface.

5.4 EIS comparison after 400th cycle

Various degradation models and their studies involve rigorous testing of the cells for them to achieve the capacity degradation of about 20 %. However, studying and testing after certain number of cycles required attention as it can also prove to be beneficial in terms of its results. After obtaining the results at 100th cycle, which provided a useful point of reference for further studies, the cells were finally tested after 400th cycles. This point of reference gives an insight of the cell every 300 cycles. The data gathered can help in predicting the cell's behavior after every 300 cycles i.e., 700, 1000, etc. Hence, for better precision modelling, the 100th cycle data can provide a useful step for every 100th cycle modelling and 400th cycle data can provide a platform for larger modelling.

Table 5. 1: Summary of R_{ct} values obtained from this study at different temperatures, different c-rates, and various number of cycles.

C-Rates		0.5C	1C	1.5C	2C	2.5C
# of Cycle	Temp.	R_{ct} (m Ω)	R_{ct} (m Ω)	R_{ct} (m Ω)	R_{ct} (m Ω)	R_{ct} (m Ω)
1 st cycle	Room Temp	7.45	2.03	1.16	19.15	1
	At 55°C	2.83	3.33	3.14	2.64	4.81
100 th cycle	Room Temp	7.46	9.22	9.42	11.2	10.83
	At 55°C	16.89	1.7	4.02	3.75	7.48
400 th cycle	Room Temp	2.54	9.15	9.75	6.78	6.38
	At 55°C	8.6	6.07	4.34	17.79	8.06

Table 5.1 above provides the data of ' R_{ct} ' at every cyclic condition tested from the 1st cycle till the 400th cycle. It is to provide a broader view into the changes occurring in the cell's internal resistance of transferring charge which is the most crucial part of any electrochemical device. At room temperature testing of the cells, the R_{ct} values show dependence on c-rates as after 400th cycle, from 0.5 C to 1.5 C, the charge-transfer resistance increases with increment in the rates. The dependency however vanishes for rates above 1.5 C as the resistance starts decreasing on these high rates. As mentioned in the previous section, the reason for this could be dendrite formation which reduces the ionic pathway in completing the charge transfer process but possesses a significant safety issue.

Figure 5.4 (a) and (b) represent the Nyquist plots of cells cycled for 400 cycles at room temperature and 55 °C, respectively. At room temperature cycling, the equivalent circuit indicates stability in their performance because of the absence of any new semicircles in the plot. However, as discussed above, the increase in resistances on higher c-rates indicates performance degradation. As pointed out by Wenpeng Cao et al. and Hossein Sharifi et al. in [86][87], respectively, the cells cycled at higher rates and those that are cycled at lower temperatures, interestingly show polarization loss and power loss resulting in higher impedances. Interestingly, the cells in Figure 5.4 (a) do show increase in internal impedances at room temperature, however, at higher rates, the opposite is occurring as R_{ct} decreased from 9.75 m Ω to 6.38 m Ω at 2.5 C rate. The cause here could

be different as mentioned earlier. In Figure 5.4 (b), the Nyquist plot of the cells cycled at higher temperatures is shown. The plots show larger charge-transfer resistance overall as compared to those at room temperature. The equivalent circuit shows two RC circuits connected to a Warburg (W) element indicating better and smoother diffusion. Hence, the temperature-based test increased the cell's internal impedance, but the elevated temperature helped in clearing out pathways for ionic species and resulted in better diffusive conditions.

Table 5.2: Summary of R_s and R_E values obtained from this study at different temperatures, different c-rates, and various number of cycles.

C-Rate		0.5 C		1 C		1.5 C		2 C		2.5 C	
No # of Cycle	Temp.	R_s (m Ω)	R_e (m Ω)	R_s (m Ω)	R_e (m Ω)	R_s (m Ω)	R_e (m Ω)	R_s (m Ω)	R_e (m Ω)	R_s (m Ω)	R_e (m Ω)
1 st cycle	Room Temp.	59.9	16.9	67.5	25.0	77.2	25.0	57.7	28.9	74.8	35.6
	At 55 °C	37.99	8.53	37.4	6.19	44.3	1.0	71.4	130	72.9	42.9
100 th cycle	Room Temp.	53	19	68.2	35.7	70.1	27.9	90.7	12.4	66.2	17.0
	At 55 °C	41.97	10.35	45.0	908	54.4	2.99	43.0	2.2	42.7	425
400 th cycle	Room Temp.	36	15	72.1	40.7	93.7	10.6	79.9	42.5	133	43.8
	At 55 °C	40	5.3	41.5	5.17	44.4	4.96	41.3	1.67	46.8	3.0

Table 5.2 summarizes the values of solution resistance, R_s , and equivalent resistance, R_e , of all the cells undergone studying from the 1st till the 400th cycle. From the values in the table, at the most extreme conditions, i.e. at the 400th cycle and at 55 °C, it can be said that the values of R_s and R_e are opposite to it each other with respect to the increasing c-rates. The values of R_s increases while that of R_e decreases. This shows that at these maximum conditions, various mechanisms are under progress as some areas are facing more resistance, most probable bulk electrolyte, while some areas are becoming more conductive and better for the cells as R_e value signifies double-layer capacitive resistance or resistance near the electrode-electrolyte interface.

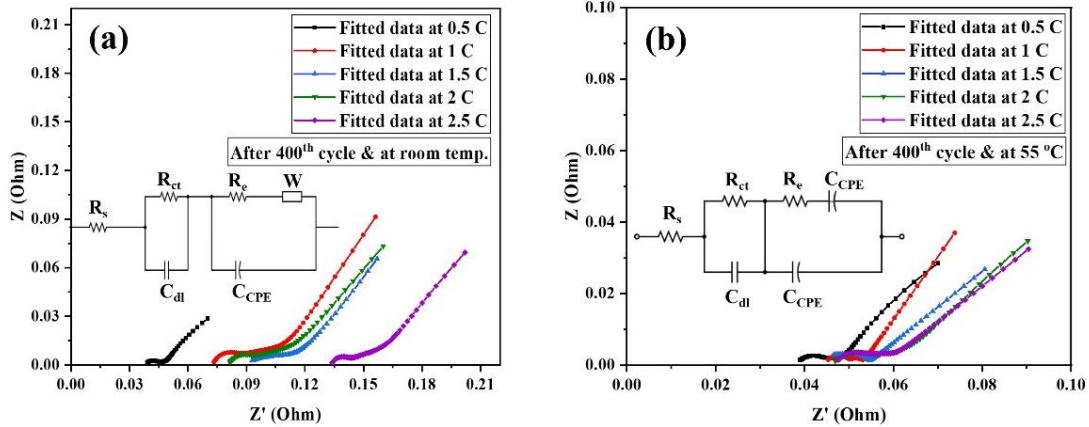


Figure 5.4: EIS comparison after 400th cycle at **a)** room temperature and **b)** 55 °C temperature.

5.5 EIS after various State of Charges (SOCs)

The State of Charge (SOC) of a cell is a crucial value as it predicts or signifies the amount of capacity the cell has with respect to its nominal capacity. It also helps in identifying the charged state or how much charge is present and how much charge has been taken out in case of discharging. SOC study reveals the voltage levels and how has the voltage window been affected upon cycling.

The experiment carried out cycling of the cells at two different c-rates, one was chosen to be the slowest of the study i.e. 0.5 C and the other was chosen to be the fastest i.e. 2.5 C. The first cell was run for a single cycle and then it was charged gradually starting from 0 to 20 % SOC and then following it up with EIS measurement after every 20 % charge. This generated five different results and showed clarity in the SOC study. The second cell was cycled for the longest cycle of this study i.e., 400 cycles. The charge/discharge rate was chosen to be the maximum of this study which was 2.5 C. This was chosen on purpose as it would give a clearer comparative study of a cell tested to its extreme conditions versus a cell which would almost act like as-manufactured cell.

Figure 5.5 (a) below shows the voltage profile of LFP cell at various states of charges (SOCs). As can be seen, the flat voltage plateau between 40 % to almost 80 % reveals a major drawback in LFP chemistry cell charging. This flat plateau makes it hard for BMS to accurately predict the SOC for LFP battery systems. This problem usually ends up the battery in overcharge

condition or at higher SOC's which could be detrimental for the battery. As seen from the figure, the voltage window spans from about 3.5 V at 20 % SOC to 3.51 V at 40 % SOC. Then, there is a slight change in its plateau and reaches 3.55 V at 60 % SOC and further increase takes it to about 3.62 V by 80 % SOC. However, as can be seen, there is a sharp rise in voltage level after 80 % SOC till 100 % SOC.

Figure 5.5 (b) and (c) show the Nyquist plots of the cell's SOC cycled at 0.5 C for a single cycle and a cell cycled at 2.5 C for 400 cycles, respectively. The cell cycled for a single cycle sets the fundamental behavior of these cells as it can be said to be the behavior depicting the as-manufactured cell. From the use of this data, any cell can be compared after certain number of cycles and or after any charge/discharge rates' cycling. From the Nyquist plot, the plots possess a semicircle in their high frequency range while a smaller semicircle is merged with it. The equivalent circuit helps in identifying the two semicircles dominating in all the plots. The circuit is fitted with C_{CPE} or a constant-phase element instead of a Warburg element reveals capacitive behavior of the cell at low frequencies, indicating the formation of double layer near the electrode-electrolyte interface [88].

As for the cell cycled till 400 cycles at 2.5 C rate, Figure 5.5 (c) reveals its Nyquist plot for all the mentioned state of charges. From the plots, it can be seen that the solution resistance, R_s , seems to decrease when SOC is increased. The plot of 100 % SOC shows large diffusion component which can be correlated to the SOC vs. Voltage graph above where higher state of charges showed sudden increase in voltages which is likely due to this significant diffusion. The plots were fitted using the equivalent circuit shown in the figure.

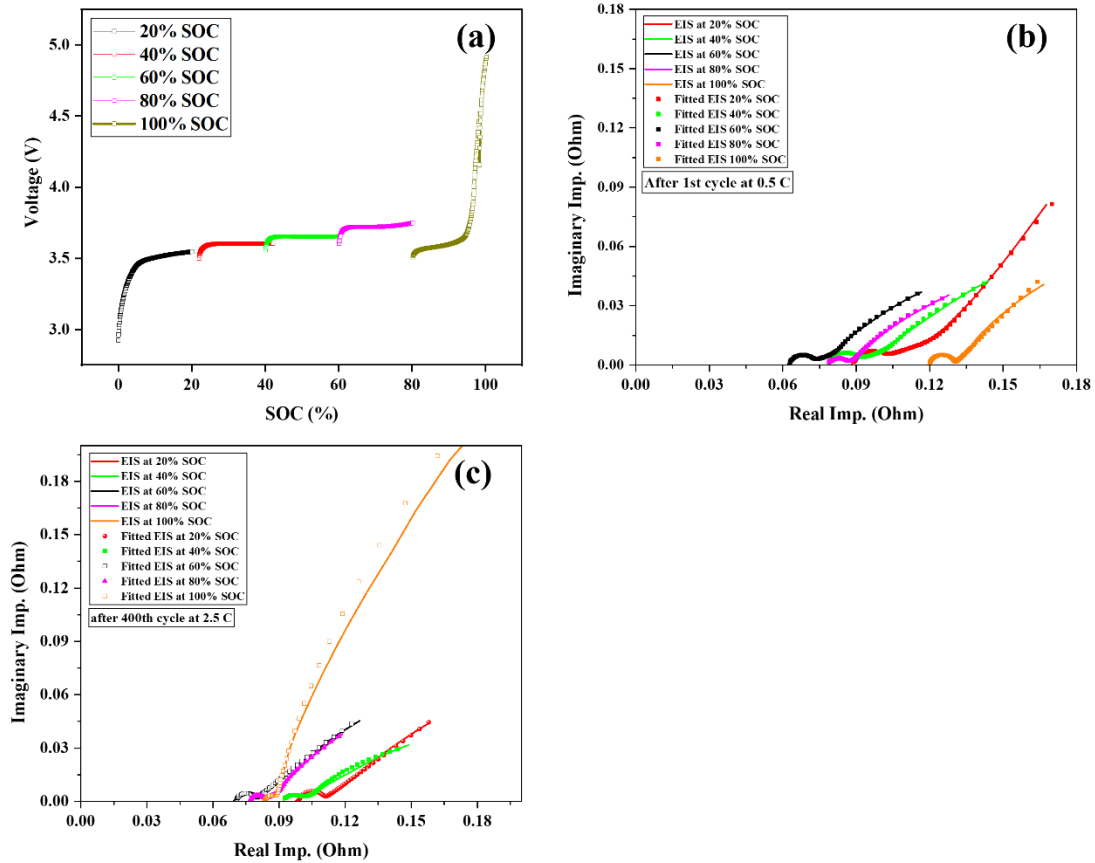


Figure 5.5: EIS study at various SOC levels **a)** SOC vs. Volt. **b)** SOC levels after 1st cycle at 0.5 C and **c)** SOC levels after 400th cycle at 2.5 C.

The cell aged for a single cycle demonstrates R_{ct} value remaining almost the same for all states of charges. From 20 % SOC to 100 % SOC, the charge-transfer resistance ranges between 9.9 m Ω to 9.6 m Ω . As for the cell cycled till 400 cycles, its SOC study reveals an R_{ct} value ranging between 10.06 m Ω at 20 % SOC to 5.13 m Ω at 100 % SOC. The values in this cell fluctuated for different states of charges but it halved by the end of charge. This value correlates with the M. Simolka *et al.* study [89] in which they found out that the LFP cells cycled below 50 % SOC degraded significantly after 300 cycles due to lower anode potential. This lower anode potential caused the formation of SEI layer on anode's surface as the electrolyte started reacting with the Li^+ inventory and started consuming it. This resulted in significant lithium loss and degraded the capacity significantly. Henceforth, the higher charge transfer resistance at 20 % SOC indicates capacity loss at the anode side as the SEI formation is limiting the charge transfers.

As discussed above, the solution resistance, R_s , showed decreasing trend for the cell cycled till 400 cycles while the cell cycled for only one cycle shows decreasing trend till 60 % SOC, but it starts increasing afterwards till 100 % SOC. However, upon closer inspection, both cells display dipping trend till 60 % SOC, but their solution/electrolyte resistance starts increasing somewhat after it. This reveals the trend studied by Andrey W. Golubkov [90] in which they found out that the main cause of thermal runaway in LFP cells are higher SOC levels which produces more vent gas than SOC levels below 50 %. Therefore, the increase in solution resistance after 60 % SOC for both cells indicates a common phenomenon which is the production of vent gases by the breaking of bonds in the bulk electrolytes.

The ' R_e ' or equivalent resistance is the resistance faced by the transportation of ions between the bulk electrolyte to the electrolyte near the electrode's surface. This resistance was present in every plot alongside ' C_{CPE} ' forming a double layer capacitance. Overall, this resistance showed no significant dependency on cycled cells and neither on any state of charges (SOCs) of any of the cells studied.

5.6 Diffusion Studies with respect to cycling of the cell cycled at 2.5 C at room temperature

After electrochemical impedance spectroscopy, the diffusion studies were carried out using the results obtained from the EIS. There are many methods to determine the diffusion coefficient from EIS data, however, almost all of them require some additional data of electrode thickness or diffusion length or the use of any other technique alongside it to determine the diffusion values [91]. However, the most used method is using the Warburg Impedance (W) to determine the diffusion coefficient (D) from its relationship. The following Equation 5.1 is derived to calculate the diffusion coefficient from the impedance data [92].

$$D = \frac{0.5 \cdot (R \cdot T)^2}{(A \cdot n^2 \cdot F^2 \cdot C \cdot \sigma)^2} \quad (5.1)$$

Here, R is the gas constant, T is the absolute temperature, A is the working electrode area, n is the number of electrons transferred in redox reaction (usually taken 1), F is the Faraday constant, C is the molar density of Li^+ in the electrode, and σ is the slope of Warburg part of EIS.

The σ can be determined through plotting the real impedance data vs. Inverse square root of ω . This shows the relationship between the Warburg impedance and σ . Once plotted, the Warburg part or the almost linear diffusion line at the low frequency is fitted linearly and its slope is determined. However, determining the working electrode's area required further mathematical calculations either through the manufacturer or other experimental methods involving post-mortem studies.

With limited data provided by the manufacturer and keeping in mind the safety hazards of post-mortem studies, a new approach was used to derive the working electrode's area. The Archimedean Principle was used to determine the length of the electrode as the cylindrical cell is rolled inside the casing in a spiral form. The length calculated was then multiplied by the width of the cell which was approximately 65 mm because the cell was 18650 model. The length was calculated using Equation 5.2 derived from Archimedean Principle:

$$L = \frac{\pi*(D^2-d^2)}{4t} \quad (5.2)$$

Here, 'D' is the outer diameter of the cell's cylinder, 'd' is the diameter of the mandrel upon which the roll is wounded upon, 't' is the total thickness of the electrodes. Using Equation 5.2 and estimating from experimental data study in [15], the thickness of the electrode ($t=313$ mm) [93], the area turns out to be, $A = 498.55$ cm².

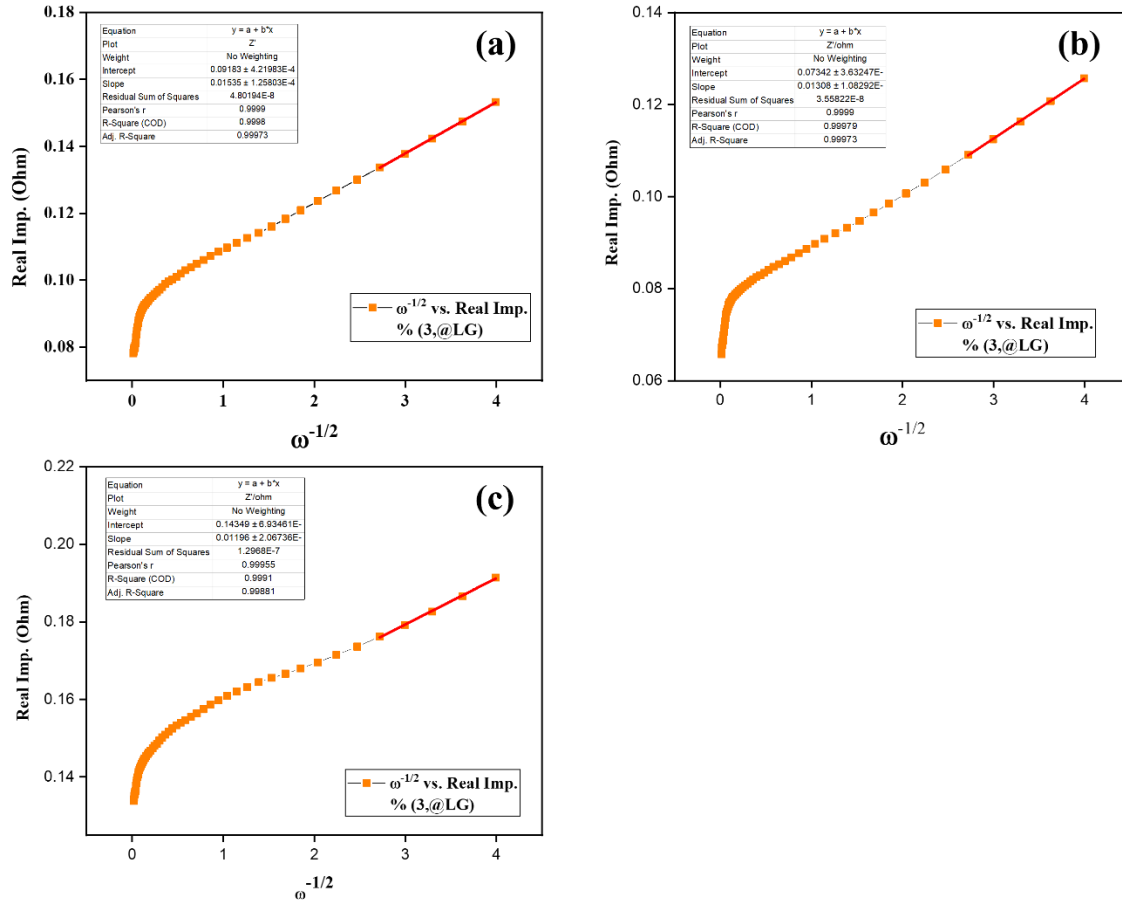


Figure 5.6: Diffusion Coefficient at 2.5 C at room temperature after **a)** 1st cycle, **b)** 100th cycle and **c)** 400th cycle.

After plotting the graph of $\omega^{-0.5}$ vs. Real Imp. (Ohm), using Origin software, the end of the graph shows the Warburg part which is selected for linear fitting. After linear fitting the data of the plot $\omega^{-0.5}$ vs. Real Imp. (Ohm), the slope of the line is measured. Figure 5.6 (a) – (c) above shows these plots of the cells undergone charging/discharging at 2.5 C rate at room temperature for 1 cycle, 100 cycles, and 400 cycles, respectively. From Figure 5.6 (a), the measured slope turned to be $\sigma = 0.0153$, for Figure 5.6 (b), the $\sigma = 0.01308$ and for Figure 5.6 (c), the $\sigma = 0.01196$.

Using the Equation 5.1, the diffusion coefficient (D) turned out to be $D = 2.133 \times 10^{-12} \text{ cm}^2/\text{s}$ for the cell cycled for a single cycle at charge/discharge rate of 2.5 C. The cell that is cycled for 100 cycles at the same rate and temperature showed $D = 2.918 \times 10^{-12} \text{ cm}^2/\text{s}$. As for the cell which

was cycled for 400 cycles at the same conditions of c-rate and temperature demonstrated diffusion coefficient $D = 3.491 \times 10^{-12} \text{ cm}^2/\text{s}$.

The values of diffusion coefficients increase with cycling the cell for a greater number of cycles. This indicates that the flow of ions inside the cell as it was cycled improved and caused a little hindrance in its mobility. The study in [94] fails to model the predictive behavior of the diffusivity of LFP cells at high c-rates as it creates confusion. However, in [95], it clarified that ionic mobility increased diffusivity although there was an increase in contact resistance in the structure of the cathode. By analyzing it through internal resistances, at 2.5 C rate, although the R_s and R_e resistances increased after 400 cycles, the charge-transfer R_{ct} , decreased. This indicates that even though the resistance in the electrolyte was increasing, the ionic species near the electrode surface faced lesser resistance and had better mobility near the electrode/electrolyte interfaces. However, the polarization effects and build-up of SEI layer caused Li^+ inventory loss as indicated by [96], could potentially degrade the cell eventually in the future as seen from the increase in internal resistances.

5.7 Diffusion studies at various c-rates

The Diffusion Coefficient study was carried out on cells cycled at various c-rates for 400 cycles (maximum number of cycles for this study) and were also compared with a fresh or as-manufactured cell (without cycling). This diffusion study would reveal the effects of charge/discharge rates on the diffusivity of the cells and how it can affect the performance.

Figure 5.7 (a) - (e) displays the plot of the inverse square root of ω vs. Real Impedance (Ohm) graph for determination of the slope σ for a cell without cycling, a cell cycled at 0.5 C, 1 C, 1.5 C, and 2 C rate for 400 cycles. These tests were performed at room temperature to better understand the underlying factors affected through charging/discharging rates. The cell cycled at 2.5 C rate has already been discussed in the above discussion.

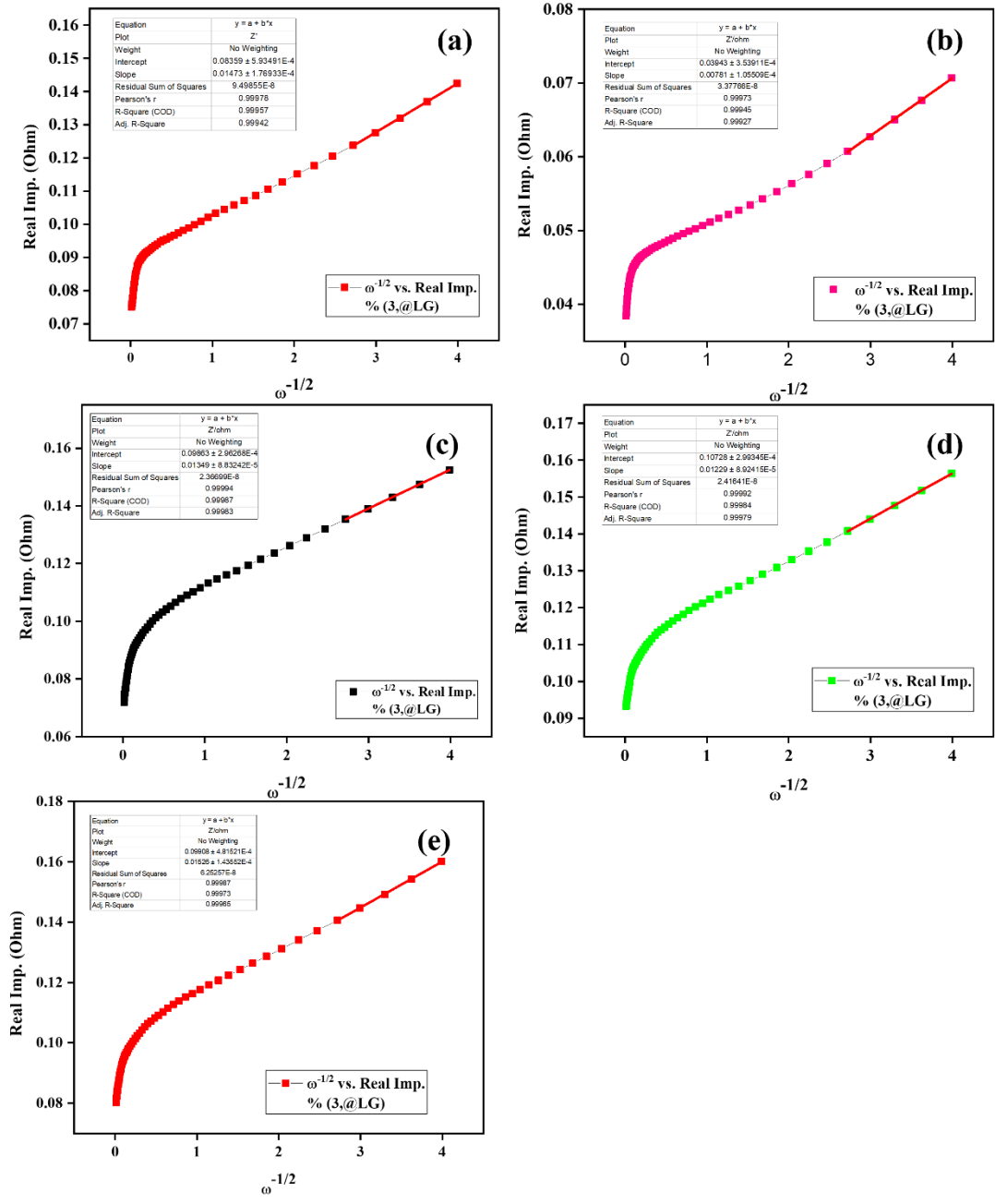


Figure 5.7: Diffusion Coefficient of cell **a)** without cycling. For cells cycled for 400 cycles **b)** at 0.5 C, **c)** at 1 C, **d)** at 1.5 C, and **e)** at 2 C.

The fresh cell upon calculation had a diffusion coefficient of $D = 1.046 \times 10^{-11} \text{ cm}^2/\text{s}$ while for cell cycled at 0.5 C rate had $D = 8.207 \times 10^{-12} \text{ cm}^2/\text{s}$, at 1 C it was $D = 2.744 \times 10^{-12} \text{ cm}^2/\text{s}$, at 1.5 C it was $D = 3.306 \times 10^{-12} \text{ cm}^2/\text{s}$, and at 2 C it was $D = 2.144 \times 10^{-12} \text{ cm}^2/\text{s}$.

The fresh cell had a higher diffusion coefficient as it hadn't undergone any cyclic disturbances or thermal runaways. As for the c-rates, the diffusion coefficient value at first decreased when the c-rate was increased from 0.5 C to 1 C rate. However, at 1.5 C rate, it increased a bit but then again showed decrement upon an increase of rate to 2 C. This fluctuating behavior of the diffusion coefficient reveals that the diffusion coefficient is somewhat independent of the charging rates and indicates the stability of LFP structure for its handling of sudden volume changes and disturbances caused by higher moving species s[97].

The performance of the cell cycled at 0.5 C was amongst the closest one to the fresh cell indicating that even though LFP's structure is stable, the lower charge/discharge rates is the most beneficial among all the charging/discharging rates as it produced the most diffusional pathways for the charges.

5.8 Summary

This chapter focuses on reviewing the results obtained from this study and to discuss its outcomes and correlations with the literature available. The results are also discussed to scientifically critique or analyze the performance of the battery cells. The results were discussed by sectioning them into different parts to better understand the influence of each factor, i.e., number of cycles, temperatures, c-rates, and SOCs on the performance of the cell. The analysis was further backup by the relevant literature and with scientific logic. Additionally, the results were further inferred from any of the already discussed sections in order to strengthen and support this analysis. All the factors were found to reveal beneficial information regarding the kinetics and the internal behaviors of the LFP cells.

CHAPTER 6: Conclusion and Future Recommendation

6.1 Conclusion

This study was carried out to analyze the kinetics and internal behavior of the LFP 18650 cylindrical cells at different numbers of cycles, temperatures, and c-rates. The study was further expanded to include the effects of State of Charge (SOCs) as well. The study revealed in general that there are various mechanisms at play when it comes to battery performance and its behaviors. Every factor and condition affects the battery differently and may or may not show a specific trend in its effectiveness. However, getting awareness of them sets the steppingstone for countering them during battery operations and their applications. Electrochemical Impedance Spectroscopy (EIS) was used to decipher the underlying behaviors and trends affecting the battery upon tinkering with external factors of battery operations.

The cyclic study at various c-rates showed different patterns in terms of the Nyquist plots obtained from EIS. The data was fitted using various types of equivalent circuits to accurately depict the trends in the Nyquist plots. The variations in the c-rates upon cycling revealed that lower and nominal c-rates caused an increase in charge transfer resistance R_{ct} and solution resistance R_s , the higher rates of 2 C and 2.5 C particularly showed a decreasing trend. This was due to better ionic mobility near the electrode's surface which produced more charge transfer events. The diffusion study confirmed this finding as the diffusion coefficient increased after cycling the cells for an increased number of cycles at higher rates. The diffusion coefficient D increased from $D = 2.133 \times 10^{-12} \text{ cm}^2/\text{s}$ after the first cycle to $D = 3.491 \times 10^{-12} \text{ cm}^2/\text{s}$ after 400 cycles at 2.5 C rate.

The temperature factor also had a significant influence on the kinetics of the LFP cells. The high temperature of 55 °C increased the activities inside a new cell by producing more electrode/electrolyte interfaces which was modelled by using R_e and C_{pe} equivalent circuit loops. The temperature also increased the overall impedance of the cell as the bulk electrolyte started to increase with cycling at higher temperatures. This could be due to polarization loss as correlated to a study and as well as due to the formation of SEI layer on anode's surface as elevated temperatures cause electrolyte's breakdown.

The cycling done at various SOC revealed a great deal of information. The cells cycled at lower SOC depicted higher charge-transfer resistances R_{ct} while the cells at higher SOC showed slight increment in their solution resistances R_s . However, cycling at lower SOC would increase the degradation rate and can cause the failure of the cell as it would the SEI formation as compared to little breakdown of the electrolytes at higher SOC.

This study comprehensively discusses and identifies how each operating factor (cycles, c-rates, temperatures, SOC) affects the battery's performance in case of its kinetic characteristics like charge-transfer resistance and diffusion coefficients. The study also highlighted how these factors impact the internal behaviors of the cells triggering various degradation mechanisms like dendrite formations, polarizations, and thermal runaways.

6.2 Limitations

The limitations of this study are that the research work carried out didn't consider large number of cycles as larger dataset could give out more information regarding the cell's internal behavior. Another limitation in this study was the verification of calculated diffusion data with the experimental data from other techniques like GITT, CV etc. Correlating with experimental data and using other techniques can strengthen the arguments presented in this paper. Lastly, the parameters like SOC need further exploration with regards to its dependency on other cyclic conditions. These are some of the main limitations of this study.

6.3 Future Recommendations

There were some suggestions for future research studies in this area which need to be tackled:

- Create a predictive model based on the electrochemical equivalent circuit model to predict the futuristic behaviors of the cells upon changing the operating conditions
- Correlate the diffusional studies with temperature-based data to better understand how change in ambient temperature affects the diffusional properties of the cells
- Study the State of Charge (SOC) with more parameters to better understand its impact on cell's performance

- Combine the kinetics models and degradation models in order to create a unified cell model which can predict any behavior
- Gather more data on changing patterns of charge transfer resistances, solutions resistances, and equivalent resistances and relate them together for any possible direct relationships

REFERENCES

- [1] Maciej Serda *et al.*, “Synteza i aktywność biologiczna nowych analogów tiosemikarbazonowych chelatorów żelaza,” *Uniwersytet śląski*, vol. 7, no. 1, pp. 343–354, 2013, doi: 10.2/JQUERY.MIN.JS.
- [2] “What does Pakistan’s energy mix look like and what is its future?” Accessed: Oct. 24, 2024. [Online]. Available: <https://www.power-technology.com/features/pakistan-energy-mix/>
- [3] “Fossil fuel consumption, 2023.” Accessed: Oct. 20, 2024. [Online]. Available: <https://ourworldindata.org/grapher/fossil-fuel-primary-energy>
- [4] S. R. Shakeel, J. Takala, and W. Shakeel, “Renewable energy sources in power generation in Pakistan,” *Renewable and Sustainable Energy Reviews*, vol. 64, pp. 421–434, Oct. 2016, doi: 10.1016/j.rser.2016.06.016.
- [5] H. Ritchie, M. Roser, and P. Rosado, “CO₂ and Greenhouse Gas Emissions,” *Our World in Data*, May 2020, Accessed: Oct. 20, 2024. [Online]. Available: <https://ourworldindata.org/co2-and-greenhouse-gas-emissions>
- [6] “14 Disadvantages of Using Fossil Fuels.” Accessed: Oct. 20, 2024. [Online]. Available: <https://www.1energysystems.com/disadvantages-of-using-fossil-fuels/>
- [7] “Renewable Energy | Advantages and Disadvantages.” Accessed: Oct. 20, 2024. [Online]. Available: <https://terrapass.com/blog/advantages-and-disadvantages-of-using-renewable-energy/>
- [8] T. Z. Ang, M. Salem, M. Kamarol, H. S. Das, M. A. Nazari, and N. Prabakaran, “A comprehensive study of renewable energy sources: Classifications, challenges and suggestions,” *Energy Strategy Reviews*, vol. 43, p. 100939, Sep. 2022, doi: 10.1016/J.ESR.2022.100939.
- [9] H. Ritchie, M. Roser, and P. Rosado, “Renewable Energy,” *Our World in Data*, 2020.
- [10] I. Renewable Energy Agency, “Tidal Energy Technology Brief,” 2014. [Online]. Available: www.irena.org
- [11] “What are the problems faced by renewable energy? - Regen Power.” Accessed: Oct. 20, 2024. [Online]. Available: <https://regenpower.com/what-are-the-problems-faced-by-renewable-energy/>
- [12] A. G. Olabi *et al.*, “Renewable energy systems: Comparisons, challenges and barriers, sustainability indicators, and the contribution to UN sustainable development goals,” *International Journal of Thermofluids*, vol. 20, p. 100498, Nov. 2023, doi: 10.1016/J.IJFT.2023.100498.

- [13] M. R. A. Bhuiyan, “Overcome the future environmental challenges through sustainable and renewable energy resources,” *Micro Nano Lett*, vol. 17, no. 14, pp. 402–416, 2022.
- [14] “Bringing Research to the Grid: Overcoming Renewable Energy Challenges – Grainger Institute for Engineering – UW–Madison.” Accessed: Oct. 20, 2024. [Online]. Available: <https://graingerinstitute.engr.wisc.edu/bringing-research-to-the-grid-overcoming-renewable-energy-challenges/>
- [15] E. Hossain, H. M. R. Faruque, M. S. H. Sunny, N. Mohammad, and N. Nawar, “A comprehensive review on energy storage systems: Types, comparison, current scenario, applications, barriers, and potential solutions, policies, and future prospects,” *Energies (Basel)*, vol. 13, no. 14, p. 3651, 2020.
- [16] “Lithium-ion Batteries | How it works, Application & Advantages.” Accessed: Oct. 20, 2024. [Online]. Available: <https://www.electricity-magnetism.org/lithium-ion-batteries/>
- [17] J. Xie and Y. C. Lu, “A retrospective on lithium-ion batteries,” *Nature Communications* 2020 11:1, vol. 11, no. 1, pp. 1–4, May 2020, doi: 10.1038/s41467-020-16259-9.
- [18] J. T. Warner, *The handbook of lithium-ion battery pack design: Chemistry, components, types, and terminology*. Elsevier, 2024.
- [19] “How Lithium-ion Batteries Work | Department of Energy.” Accessed: Oct. 20, 2024. [Online]. Available: <https://www.energy.gov/energysaver/articles/how-lithium-ion-batteries-work>
- [20] “Lithium-Ion Battery Pack Design & Manufacturing Q&A.” Accessed: Oct. 20, 2024. [Online]. Available: <https://holobattery.com/lithium-ion-battery-pack-design-manufacturing-qa/>
- [21] B. Writer, “Lithium-ion batteries,” *A Machine-Generated Summary of Current Research. Cham: Springer International Publishing*, vol. 3, 2019.
- [22] D. Deng, “Li-ion batteries: basics, progress, and challenges,” *Energy Sci Eng*, vol. 3, no. 5, pp. 385–418, 2015.
- [23] “Lithium-Ion Battery Chemistry: How to Compare? | EnergySage.” Accessed: Oct. 20, 2024. [Online]. Available: <https://www.energysage.com/energy-storage/types-of-batteries/comparing-lithium-ion-battery-chemistries/>
- [24] “NMC vs LFP: safety and performance in operation - PowerUp.” Accessed: Oct. 20, 2024. [Online]. Available: <https://powerup-technology.com/nmc-vs-lfp-safety-and-performance-in-operation/>
- [25] “EV battery types explained: Lithium-ion vs LFP pros & cons.” Accessed: Oct. 20, 2024. [Online]. Available: <https://www.whichcar.com.au/advice/ev-battery-types-explained-electric-car-pros-cons>

- [26] T. Wulandari, D. Fawcett, S. B. Majumder, and G. E. J. Poinern, “Lithium-based batteries, history, current status, challenges, and future perspectives,” *Battery Energy*, vol. 2, no. 6, p. 20230030, Nov. 2023, doi: 10.1002/BTE2.20230030.
- [27] “Chemical kinetics | Definition, Equations, & Facts | Britannica.” Accessed: Oct. 20, 2024. [Online]. Available: <https://www.britannica.com/science/chemical-kinetics>
- [28] C. Brett, “Electrochemical Impedance Spectroscopy for Characterization of Electrochemical Sensors and Biosensors,” *ECS Trans.*, vol. 13, no. 13, p. 67, 2008.
- [29] Z. Gao, H. Xie, X. Yang, W. Niu, S. Li, and S. Chen, “The Dilemma of C-Rate and Cycle Life for Lithium-Ion Batteries under Low Temperature Fast Charging,” *Batteries*, vol. 8, no. 11, Nov. 2022, doi: 10.3390/batteries8110234.
- [30] D. Qu, W. Ji, and H. Qu, “Probing process kinetics in batteries with electrochemical impedance spectroscopy,” *Communications Materials 2022 3:1*, vol. 3, no. 1, pp. 1–9, Sep. 2022, doi: 10.1038/s43246-022-00284-w.
- [31] J. Mitali, S. Dhinakaran, and A. A. Mohamad, “Energy storage systems: a review,” *Energy Storage and Saving*, vol. 1, no. 3, pp. 166–216, Sep. 2022, doi: 10.1016/J.ENSS.2022.07.002.
- [32] G. Zhao, X. Wang, and M. Negnevitsky, “Connecting battery technologies for electric vehicles from battery materials to management,” *iScience*, vol. 25, no. 2, p. 103744, Feb. 2022, doi: 10.1016/J.ISCI.2022.103744.
- [33] P. Breeze, “Power generation technologies,” *Power Generation Technologies*, pp. 1–449, Jan. 2019, doi: 10.1016/C2017-0-03267-6.
- [34] T. R. (Thomas R. Crompton, *Battery reference book / T.R. Crompton*. Accessed: Oct. 21, 2024. [Online]. Available: <http://www.sciencedirect.com:5070/book/9780750646253/battery-reference-book>
- [35] T. Wulandari, D. Fawcett, S. B. Majumder, and G. E. J. Poinern, “Lithium-based batteries, history, current status, challenges, and future perspectives,” *Battery Energy*, vol. 2, no. 6, p. 20230030, Nov. 2023, doi: 10.1002/BTE2.20230030.
- [36] U. Chikezie and Z. Chen, “Literature Review of Energy Storage for Power System Economics,” *2020 IEEE 3rd International Conference on Renewable Energy and Power Engineering, REPE 2020*, pp. 67–72, Oct. 2020, doi: 10.1109/REPE50851.2020.9253910.
- [37] S. Koochi-Fayegh and M. A. Rosen, “A review of energy storage types, applications and recent developments,” *J Energy Storage*, vol. 27, p. 101047, Feb. 2020, doi: 10.1016/J.EST.2019.101047.
- [38] “Internet Archive: Service Availability.” Accessed: Oct. 21, 2024. [Online]. Available: <https://archive.org/download/CROMPTONT.R.2000.BatteryReferenceBook3rdEd./CRO>

MPTON%2C%20T.%20R.%20%282000%29.%20Battery%20Reference%20Book%20%283rd%20ed.%29.pdf

- [39] Y. Zhu, T. Gao, X. Fan, F. Han, and C. Wang, “Electrochemical Techniques for Intercalation Electrode Materials in Rechargeable Batteries,” *Acc Chem Res*, vol. 50, no. 4, pp. 1022–1031, Apr. 2017, doi: 10.1021/ACS.ACCOUNTS.7B00031/ASSET/IMAGES/LARGE/AR-2017-00031J_0006.JPEG.
- [40] F. Xie, O. Czogalla, and S. Naumann, “Lithium Battery Model Development and Application in Simulation of the Energy Consumption of Electric Bus Running,” *IFAC-PapersOnLine*, vol. 53, no. 2, pp. 14230–14235, Jan. 2020, doi: 10.1016/J.IFACOL.2020.12.1153.
- [41] D. I. Stroe, A. Zaharof, and F. Iov, “Power and Energy Management with Battery Storage for a Hybrid Residential PV-Wind System – A Case Study for Denmark,” *Energy Procedia*, vol. 155, pp. 464–477, Nov. 2018, doi: 10.1016/J.EGYPRO.2018.11.033.
- [42] “LEAD-ACID BATTERY AGING AND STATE OF HEALTH.” Accessed: Oct. 21, 2024. [Online]. Available: <https://studylib.net/doc/18915515/lead-acid-battery-aging-and-state-of-health>
- [43] K. Vignarooban *et al.*, “State of health determination of sealed lead acid batteries under various operating conditions,” *Sustainable Energy Technologies and Assessments*, vol. 18, pp. 134–139, Dec. 2016, doi: 10.1016/J.SETA.2016.10.007.
- [44] V. Pop, H. J. Bergveld, P. H. L. Notten, and P. P. L. Regtien, “State-of-the-art of battery state-of-charge determination,” *Meas Sci Technol*, vol. 16, no. 12, Dec. 2005, doi: 10.1088/0957-0233/16/12/R01.
- [45] J. Albers, “Heat tolerance of automotive lead-acid batteries,” *J Power Sources*, vol. 190, no. 1, pp. 162–172, May 2009, doi: 10.1016/J.JPOWSOUR.2008.12.105.
- [46] M. Dubarry and B. Y. Liaw, “Identify capacity fading mechanism in a commercial LiFePO₄ cell,” *J Power Sources*, vol. 194, no. 1, pp. 541–549, Oct. 2009, doi: 10.1016/J.JPOWSOUR.2009.05.036.
- [47] F. Huet, “A review of impedance measurements for determination of the state-of-charge or state-of-health of secondary batteries,” *J Power Sources*, vol. 70, no. 1, pp. 59–69, Jan. 1998, doi: 10.1016/S0378-7753(97)02665-7.
- [48] Z. Yanhui, S. Wenji, L. Shili, L. Jie, and F. Ziping, “A critical review on state of charge of batteries,” *Journal of Renewable and Sustainable Energy*, vol. 5, no. 2, Mar. 2013, doi: 10.1063/1.4798430.
- [49] T. Rauhala, K. Jalkanen, T. Romann, E. Lust, N. Omar, and T. Kallio, “Low-temperature aging mechanisms of commercial graphite/LiFePO₄ cells cycled with a simulated electric

- vehicle load profile—A post-mortem study,” *J Energy Storage*, vol. 20, pp. 344–356, Dec. 2018, doi: 10.1016/J.EST.2018.10.007.
- [50] J. Wang *et al.*, “Cycle-life model for graphite-LiFePO₄ cells,” *J Power Sources*, vol. 196, no. 8, pp. 3942–3948, Apr. 2011, doi: 10.1016/J.JPOWSOUR.2010.11.134.
- [51] S. Sagaria, M. van der Kam, and T. Boström, “Vehicle-to-grid impact on battery degradation and estimation of V2G economic compensation,” *Appl Energy*, vol. 377, Jan. 2025, doi: 10.1016/j.apenergy.2024.124546.
- [52] S. S. Choi and H. S. Lim, “Factors that affect cycle-life and possible degradation mechanisms of a Li-ion cell based on LiCoO₂,” *J Power Sources*, vol. 111, no. 1, pp. 130–136, Sep. 2002, doi: 10.1016/S0378-7753(02)00305-1.
- [53] Y. C. Chuang and Y. L. Ke, “High efficiency battery charger with a buck zero-current-switching pulse-width-modulated converter,” *IET Power Electronics*, vol. 1, no. 4, pp. 433–444, 2008, doi: 10.1049/IET-PEL:20070215.
- [54] “Bor Yann Liaw | Idaho National Laboratory - Academia.edu.” Accessed: Oct. 21, 2024. [Online]. Available: <https://inl.academia.edu/BorYannLiaw/CurriculumVitae>
- [55] M. G. Simoes, S. Mohagheghi, P. Siano, P. Palensky, and X. Yu, “Advances in information technology for Smart Grids,” *IECON Proceedings (Industrial Electronics Conference)*, pp. 36–41, 2013, doi: 10.1109/IECON.2013.6699108.
- [56] H. Bindner, T. Cronin, J. F. Manwell, U. Abdulwahid, I. Baring-Gould, and U. Abdulwaliid, “Lifetime Modelling of Lead Acid Batteries Title: Lifetime Modelling of Lead Acid Batteries Department: YEA, VES,” vol. 1515, no. April, p. Risø Nat. Lab., 2005, Accessed: Oct. 21, 2024. [Online]. Available: www.risoe.dk
- [57] و. الفراتي, “A gateway framework for System of Systems,” *IECON 2016 - 42nd Annual Conference of the IEEE Industrial Electronics Society*, Jan. 2016, Accessed: Oct. 21, 2024. [Online]. Available: https://www.academia.edu/86335540/A_gateway_framework_for_System_of_Systems
- [58] V. Etacheri, R. Marom, R. Elazari, G. Salitra, and D. Aurbach, “Challenges in the development of advanced Li-ion batteries: A review,” *Energy Environ Sci*, vol. 4, no. 9, pp. 3243–3262, Sep. 2011, doi: 10.1039/C1EE01598B.
- [59] B. Shi, B. Han, H. Xie, Y. Kang, and Q. Zhang, “C-rate related diffusion process of the graphite electrode by in situ experiment and analysis,” *Electrochim Acta*, vol. 378, p. 138151, May 2021, doi: 10.1016/J.ELECTACTA.2021.138151.
- [60] MTI corporation, “8 Channel Battery Analyzer (0.005 -1 mA, up to 5V) w/ Laptop Software & Optional WIFI Control”, Accessed: Oct. 20, 2024. [Online]. Available: <https://www.mtixtl.com/8ChannelsBatteryAnalyzer-BST8-WA.aspx>

- [61] “Understanding The Battery Charging Modes: Constant Current and Constant Voltage Modes,” *EV Charging*, May 2024.
- [62] J. J. Chen, F. C. Yang, C. C. Lai, Y. S. Hwang, and R. G. Lee, “A high-efficiency multimode Li-Ion battery charger with variable current source and controlling previous-stage supply voltage,” *IEEE Transactions on Industrial Electronics*, vol. 56, no. 7, pp. 2469–2478, 2009, doi: 10.1109/TIE.2009.2018435.
- [63] Discover innovative battery solution, “Constant Current Charging Method of Battery Charging Discover Battery”, Accessed: Oct. 20, 2024. [Online]. Available: <https://discoverbattery.com/support/learning-center/learning-center-articles/what-is-constant-current-cc-charging>
- [64] S. H. Hwang, Y. Chen, H. Zhang, K. Y. Lee, and D. H. Kim, “Reconfigurable hybrid resonant topology for constant current/voltage wireless power transfer of electric vehicles,” *Electronics (Switzerland)*, vol. 9, no. 8, pp. 1–13, Aug. 2020, doi: 10.3390/ELECTRONICS9081323.
- [65] H. Liu *et al.*, “An analytical model for the CC-CV charge of Li-ion batteries with application to degradation analysis,” *J Energy Storage*, vol. 29, p. 101342, Jun. 2020, doi: 10.1016/J.EST.2020.101342.
- [66] A. C. Lazanas and M. I. Prodromidis, “Electrochemical Impedance Spectroscopy—A Tutorial,” *ACS Measurement Science Au*, vol. 3, no. 3, pp. 162–193, Jun. 2023, doi: 10.1021/ACSMEASURESCIAU.2C00070/ASSET/IMAGES/LARGE/TG2C00070_0032.JPEG.
- [67] H. S. Magar, R. Y. A. Hassan, and A. Mulchandani, “Electrochemical impedance spectroscopy (Eis): Principles, construction, and biosensing applications,” Oct. 01, 2021, *MDPI*. doi: 10.3390/s21196578.
- [68] K. Liu, K. Li, Q. Peng, and C. Zhang, “A brief review on key technologies in the battery management system of electric vehicles,” *Frontiers of Mechanical Engineering*, vol. 14, no. 1, pp. 47–64, Mar. 2019, doi: 10.1007/S11465-018-0516-8/METRICS.
- [69] R. J. Wang, Y. H. Pan, Y. Le Nian, and W. L. Cheng, “Study on dynamic thermal control performance of positive temperature coefficient (PTC) material based on a novel heat transfer model considering internal heat transfer,” *Appl Therm Eng*, vol. 165, p. 114452, Jan. 2020, doi: 10.1016/J.APPLTHERMALENG.2019.114452.
- [70] A. C. Lazanas and M. I. Prodromidis, “Electrochemical Impedance Spectroscopy—A Tutorial,” *ACS Measurement Science Au*, vol. 3, no. 3, pp. 162–193, Jun. 2023, doi: 10.1021/ACSMEASURESCIAU.2C00070.
- [71] “Low-Cost Design of Poultry Egg Incubator with W1209 Digital Temperature Controller | Request PDF.” Accessed: Oct. 22, 2024. [Online]. Available: https://www.researchgate.net/publication/341114331_Low-Cost_Design_of_Poultry_Egg_Incubator_with_W1209_Digital_Temperature_Controller

- [72] K. T. Aminu *et al.*, “NTC Thermistor Performance and Linearization of its Temperature-Resistance Characteristics Using Electronic Circuit,” *International Journal of Advances in Scientific Research and Engineering*, vol. 06, no. 08, pp. 35–49, 2020, doi: 10.31695/IJASRE.2020.33854.
- [73] “5. Constant Current and Constant Voltage Charging of Wireless Power Transfer System Based on Three-Coil Structure | Request PDF (researchgate.net) - Google Search.” Accessed: Oct. 22, 2024. [Online]. Available: [https://www.google.com/search?q=5.+Constant+Current+and+Constant+Voltage+Charging+of+Wireless+Power+Transfer+System+Based+on+Three-Coil+Structure+%7C+Request+PDF+\(researchgate.net\)&rlz=1C1ONGR_en-GBDE1023DE1023&oq=5.%09Constant+Current+and+Constant+Voltage+Charging+of+Wireless+Power+Transfer+System+Based+on+Three-Coil+Structure+%7C+Request+PDF+\(researchgate.net\)&gs_lcrp=EgZjaHJvbWUqBggAEEUYOzIGCAAQRrg7MgYIARBFGEQSAQc4MDNqMGo3qAIIsAIB&sourceid=chrome&ie=UTF-8](https://www.google.com/search?q=5.+Constant+Current+and+Constant+Voltage+Charging+of+Wireless+Power+Transfer+System+Based+on+Three-Coil+Structure+%7C+Request+PDF+(researchgate.net)&rlz=1C1ONGR_en-GBDE1023DE1023&oq=5.%09Constant+Current+and+Constant+Voltage+Charging+of+Wireless+Power+Transfer+System+Based+on+Three-Coil+Structure+%7C+Request+PDF+(researchgate.net)&gs_lcrp=EgZjaHJvbWUqBggAEEUYOzIGCAAQRrg7MgYIARBFGEQSAQc4MDNqMGo3qAIIsAIB&sourceid=chrome&ie=UTF-8)
- [74] J. Lukić and D. Denić, “A novel design of an ntc thermistor linearization circuit,” *Metrology and Measurement Systems*, vol. 22, no. 3, pp. 351–362, Sep. 2015, doi: 10.1515/MMS-2015-0035.
- [75] H. S. Magar, R. Y. A. Hassan, and A. Mulchandani, “Electrochemical impedance spectroscopy (Eis): Principles, construction, and biosensing applications,” *Sensors*, vol. 21, no. 19, Oct. 2021, doi: 10.3390/S21196578.
- [76] W. Weppner and R. A. Huggins, “Determination of the Kinetic Parameters of Mixed-Conducting Electrodes and Application to the System Li₃Sb,” *J Electrochem Soc*, vol. 124, no. 10, pp. 1569–1578, Oct. 1977, doi: 10.1149/1.2133112/XML.
- [77] S. Q. Liu, S. C. Li, K. L. Huang, B. L. Gong, and G. Zhang, “Kinetic study on Li_{2.8}(V_{0.9}Ge_{0.1})₂(PO₄)₃ by EIS measurement,” *J Alloys Compd*, vol. 450, no. 1–2, pp. 499–504, Feb. 2008, doi: 10.1016/J.JALLCOM.2006.11.131.
- [78] P. Keil and A. Jossen, “Charging protocols for lithium-ion batteries and their impact on cycle life—An experimental study with different 18650 high-power cells,” *J Energy Storage*, vol. 6, pp. 125–141, May 2016, doi: 10.1016/J.EST.2016.02.005.
- [79] B. A. Mei, O. Munteshari, J. Lau, B. Dunn, and L. Pilon, “Physical Interpretations of Nyquist Plots for EDLC Electrodes and Devices,” *Journal of Physical Chemistry C*, vol. 122, no. 1, pp. 194–206, Jan. 2018, doi: 10.1021/acs.jpcc.7b10582.
- [80] A. C. Lazanas and M. I. Prodromidis, “Electrochemical Impedance Spectroscopy—A Tutorial,” Jun. 21, 2023, *American Chemical Society*. doi: 10.1021/acsmeasuresciau.2c00070.
- [81] Y. Preger *et al.*, “Degradation of Commercial Lithium-Ion Cells as a Function of Chemistry and Cycling Conditions,” *J Electrochem Soc*, vol. 167, no. 12, p. 120532, Jan. 2020, doi: 10.1149/1945-7111/abae37.

- [82] T. Waldmann, B. I. Hogg, and M. Wohlfahrt-Mehrens, "Li plating as unwanted side reaction in commercial Li-ion cells – A review," Apr. 30, 2018, *Elsevier B.V.* doi: 10.1016/j.jpowsour.2018.02.063.
- [83] A. Javaid, H. A. Khalid, S. A. Abbas Kazmi, and G. Ali, "Analysis of lithium diffusion and overpotential in lithium nickel cobalt aluminum oxide based lithium ion cells," *Journal of Electroanalytical Chemistry*, vol. 952, Jan. 2024, doi: 10.1016/j.jelechem.2023.117991.
- [84] B. Fang and L. Binder, "A modified activated carbon aerogel for high-energy storage in electric double layer capacitors," *J Power Sources*, vol. 163, no. 1 SPEC. ISS., pp. 616–622, Dec. 2006, doi: 10.1016/j.jpowsour.2006.09.014.
- [85] K. H. An *et al.*, "Electrochemical Properties of High-Power Supercapacitors Using Single-Walled Carbon Nanotube Electrodes**."
- [86] W. Cao, J. Li, and Z. Wu, "Cycle-life and degradation mechanism of LiFePO₄-based lithium-ion batteries at room and elevated temperatures," *Ionics (Kiel)*, vol. 22, no. 10, pp. 1791–1799, Oct. 2016, doi: 10.1007/s11581-016-1703-4.
- [87] H. Sharifi, B. Mosallanejad, M. Mohammadzad, S. M. Hosseini-Hosseini, and S. Ramakrishna, "Cycling performance of LiFePO₄/graphite batteries and their degradation mechanism analysis via electrochemical and microscopic techniques," *Ionics (Kiel)*, vol. 28, no. 1, pp. 213–228, Jan. 2022, doi: 10.1007/s11581-021-04258-9.
- [88] K. H. An *et al.*, "Electrochemical Properties of High-Power Supercapacitors Using Single-Walled Carbon Nanotube Electrodes**."
- [89] M. Simolka, J. F. Heger, H. Kaess, I. Biswas, and K. A. Friedrich, "Influence of cycling profile, depth of discharge and temperature on commercial LFP/C cell ageing: post-mortem material analysis of structure, morphology and chemical composition," *J Appl Electrochem*, vol. 50, no. 11, pp. 1101–1117, Nov. 2020, doi: 10.1007/s10800-020-01465-6.
- [90] A. W. Golubkov *et al.*, "Thermal runaway of commercial 18650 Li-ion batteries with LFP and NCA cathodes - Impact of state of charge and overcharge," *RSC Adv*, vol. 5, no. 70, pp. 57171–57186, 2015, doi: 10.1039/c5ra05897j.
- [91] T. Q. Nguyen and C. Breitkopf, "Determination of Diffusion Coefficients Using Impedance Spectroscopy Data," *J Electrochem Soc*, vol. 165, no. 14, pp. E826–E831, 2018, doi: 10.1149/2.1151814jes.
- [92] "CRC_Handbook_of_Thermophysical_and_Therm".
- [93] T. Waldmann, R. G. Scurtu, K. Richter, and M. Wohlfahrt-Mehrens, "18650 vs. 21700 Li-ion cells – A direct comparison of electrochemical, thermal, and geometrical properties," *J Power Sources*, vol. 472, Oct. 2020, doi: 10.1016/j.jpowsour.2020.228614.

- [94] S. Taslimi Taleghani, B. Marcos, and G. Lantagne, "Modeling and simulation of a commercial graphite–LiFePO₄ cell in a full range of C-rates," *J Appl Electrochem*, vol. 48, no. 12, pp. 1389–1400, Dec. 2018, doi: 10.1007/s10800-018-1239-6.
- [95] E. R. Logan *et al.*, "The Effect of LiFePO₄ Particle Size and Surface Area on the Performance of LiFePO₄ /Graphite Cells," *J Electrochem Soc*, vol. 169, no. 5, p. 050524, May 2022, doi: 10.1149/1945-7111/ac6aed.
- [96] J. Geng *et al.*, "A review of graphene-decorated LiFePO₄ cathode materials for lithium-ion batteries," Nov. 01, 2022, *Springer Science and Business Media Deutschland GmbH*. doi: 10.1007/s11581-022-04679-0.
- [97] P. P. Prosini, M. Lisi, D. Zane, and M. Pasquali, "Determination of the chemical diffusion coefficient of lithium in LiFePO₄." [Online]. Available: www.elsevier.com/locate/ssi

LIST OF PUBLICATION

Full-length article title: Kinetic Analysis and Diffusion Coefficient Measurement of Life po4 cells using EIS Technique.

Journal: ACS publications

Manuscript number: EC-2024-00196r

Date of submission: 2nd December 2024

Current Status: Under Review

The screenshot displays the ACS Paragon Plus submission interface. At the top, there is a navigation bar with the ACS Publications logo and the text 'ACS Paragon Plus Powered by ScholarOne Manuscripts™'. Below this, a blue banner contains the ACS Publications logo and the text 'ACS Paragon Plus'. A message states: 'The ACS Publishing Center will soon be your new gateway to all ACS publishing services. Take control. Bookmark and use <https://publish.acs.org> now to ensure the best experience.'

The main content area is titled 'Welcome to ACS Paragon Plus'. It features a section for submitting a new manuscript, with a dropdown menu labeled 'Select a journal...'. Below this, there are tabs for 'My Authoring Activity' and 'My Reviewing Assignments'. The 'My Authoring Activity' tab is active, showing a list of submissions. The first submission is highlighted in blue and is in the 'Submitted to Editorial Office' stage. It is sorted by 'Date' and has a filter input field. The submission details are as follows:

2	Submitted to Editorial Office	Sort By	Date	↓
1	ACS Electrochemistry			
	Kinetic analysis and diffusion coefficient measurements of LiFePO4 cells using EIS technique			
	Manuscript ID: ec-2024-00196r			
	Status: Under Review			
	Submitted on 02 December 2024			
	Manuscript	Cover Letter		